João Paulo Caseiro Baixinho

Degree in Cell and Molecular Biology

Development of curcumin lipid formulations for food applications: transport, permeability and safety evaluation on a mucus-secreting intestinal epithelial cell model

Dissertation to obtain master degree in Biotechnology

Supervisor: Ana Matias, PhD, IBET
Co-Supervisor: Vanessa Gonçalves, PhD, IBET

FACULDADE DE CIÊNCIAS E TECNOLOGIA
UNIVERSIDADE NOVA DE LISBOA

September 2018

João Paulo Caseiro Baixinho

Degree in Cell and Molecular Biology

Development of curcumin lipid formulations for food applications: transport, permeability and safety evaluation on a mucus-secreting intestinal epithelial cell model

Dissertation to obtain master degree in Biotechnology

Supervisor: Ana Matias, PhD, IBET
Co-Supervisor: Vanessa Gonçalves, PhD, IBET

September 2018

“Copyright”

Development of curcumin lipid formulations for food applications: transport, permeability and safety evaluation on a mucus-secreting intestinal epithelial cell model.

João Paulo Caseiro Baixinho, FCT/UNL e UNL

Acknowledgments

Gostaria de agradecer a todos as pessoas que, direta ou indiretamente, contribuíram para a realização deste trabalho.

Em primeiro lugar, à Doutora Ana Matias, por me ter dado a oportunidade de desenvolver este trabalho no laboratório de Nutracêuticos e Libertação Controlada. Agradeço toda a orientação prestada, a sua preocupação e apoio constante.

À Vanessa Gonçalves, agradeço toda a orientação, conhecimento e apoio. Obrigado acima de tudo pela tua disponibilidade.

Agradeço a todos os membros e colegas do laboratório de Nutracêuticos e Libertação Controlada e de uma forma especial:

À Joana Guerreiro, por toda a ajuda prestada nos ensaios celulares. Muito obrigada pela tua disponibilidade e paciência.

Ao Agostinho Alexandre, por todos os momentos passados juntos. Pelas críticas e conhecimento transmitido. Obrigada pela tua preocupação e companhia.

À Liliana Rodrigues por estar sempre disponível para ouvir as minhas dúvidas e problemas. Obrigado pelo teu apoio e assertividade!

À Carolina, Naiara, Ana Nunes e Ana Roda. Obrigada pela vossa amizade e preocupação.

Agradeço de uma forma especial aos meus amigos e colegas, Nuno, Pedro e Miguel por todo o apoio e companhia nos momentos mais difíceis. Um especial obrigado ao Miguel pela entreajuda e companheirismo nos mais diversos momentos. Sem dúvida que contigo isto ficou mais fácil!

Um especial obrigado ao Tiago Filipe “Baladeiro” e ao João “Potter” Ribeiro por transformarem cada dia de Sporting num dia de descontração, diversão e amizade. Obrigado pelas distrações que precisava.

O agradecimento mais importante dirige-se a toda a minha família, em especial aos meus pais, por todos os sacrifícios e obstáculos ultrapassados para me oferecerem a oportunidade de completar mais uma importante etapa da minha vida. Tudo o que sou hoje é graças a vós. Muito obrigado.

Preface

This work was performed at the Nutraceuticals and Bioactives process technology laboratory, Instituto de Biologia Experimental e Tecnológica (IBET), under the scope of the project NanoMaxiSafe (PTDC/AGRTEC/5215/2014), financially supported by the Fundação para a Ciência e Tecnologia (FCT), Portugal. Part of the work presented in this thesis has been included in poster communications during the year.

Poster communication:

- ✓ J. N. Guerreiro**, J. C. Baixinho** et al. Improving bioactives intestinal absorption using lipidic nanodelivery systems in food applications: evaluation of toxicity and bioavailability. 1st UNGAP Meeting, 2018, Leuven, Belgium.

- ✓ J. N. Guerreiro**, J. C. Baixinho** et al. Cytotoxicity and bioavailability evaluation using an in vitro triple co-culture intestinal cell culture: improving bioactives absorption using novel lipidic nanodelivery systems in food applications. BioBarriers, 27st-28st August 2018, Saarbrucken, Germany.

Abstract

Curcumin is the main phenolic pigment extracted from turmeric, the powdered rhizome of *Curcuma longa*. It has been shown to exhibit antioxidant, antimicrobial, anti-inflammatory and anticarcinogenic activities however as health promoting agent, curcumin, is limited by its poor solubility in aqueous solution and its low bioavailability and therefore cannot be widely used in food and pharmaceutical processing industry.

The challenge addressed in this work was to produce curcumin formulations to enhance its characteristics and evaluate its permeability, transport and cytotoxicity on a stablished *in vitro* cell co-culture model that mimics the intestinal epithelium.

Solid lipid nanoparticles (SLN) and microparticles (SLM) have been visualised as a promising platform on development of formulations for food applications. Since traditional production methods possess a series of limitations, the processing by "green technologies" like supercritical carbon dioxide ($scCO_2$) has been widely investigated. Through Particles from Gas Saturated Solutions (PGSS®) process, beeswax microparticles loaded with curcumin (9:1 (w/w)) were produced and characterized in terms of physicochemical properties: size, morphology, curcumin content and particles dispersion index. Operation process parameters were optimized and defined via response surface methodology and the best response was achieved at 160 bar, 73°C and 10% curcumin load. Under these conditions, encapsulation efficiency was 89.75 ± 2.23 % with a curcumin load of 8.98 % (w/w). Curcumin formulations underwent a digestive process and were tested for their cytotoxicity in Caco-2 monolayer.

A triple co-culture has been established and characterized for use as an *in vitro* intestinal model. To closely mimic the intestinal epithelium the production of mucus by the HT29-MTX-E12 cell line cultured together with the Caco-2 enterocytes and M-cells like phenotype was observed. The model was used to evaluate the transport and permeability of free and encapsulated curcumin and its permeability was stablished as a value of 1.0×10^{-7} cm/s.

Keywords:

Curcumin, Caco-2, PGSS®, triple co-culture model, solid lipid particles.

Resumo

A curcumina, o principal pigmento fenólico extraído da curcuma apresenta diversas propriedades antioxidantes, antimicrobianas, anti-inflamatórias e anticarcinogénicas, no entanto a sua utilização é limitada pela sua fraca solubilidade e biodisponibilidade no epitélio intestinal humano, o que consequentemente provoca a sua limitada utilização na indústria alimentar e farmacêutica.

O desafio abordado neste trabalho foi produzir formulações de curcumina para despoletar as suas características e avaliar a sua permeabilidade, transporte e citotoxicidade num modelo de co-cultura celular estabelecido para mimetizar o epitélio intestinal.

Partículas lipídicas solidas (SLP) têm sido visualizadas como uma plataforma promissora no desenvolvimento de formulações para aplicações alimentares. Como os métodos tradicionais de produção possuem uma série de limitações, o processamento por "tecnologias verdes" como o dióxido de carbono supercrítico ($scCO_2$) tem sido amplamente investigado. Através do processo Particles from Gas Saturated Solutions (PGSS®), micropartículas de cera de abelha carregadas com curcumina (9:1 (m/m)) foram produzidas e caracterizadas em termos das suas qualidades físico-químicas: morfologia, tamanho, quantidade de curcumina e índice de polidispersão. O processo de produção foi otimizado e definido através da metodologia de superfície de resposta sendo que a melhor resposta foi obtida a 160 bar, 73 °C e 10 % de curcumina. Nestas condições, a eficiência de encapsulação foi de 89,75 ± 2,23 % com uma encapsulação de 8,98 %. As micropartículas foram submetidas a um processo digestivo e testadas quanto à sua citotoxicidade em monocamada de células Caco-2.

Para mimetizar o epitélio intestinal uma co-cultura tripla foi estabelecida e caracterizada observando-se a produção de muco pela linha celular HT29-MTX-E12 cultivada em conjunto com os enterócitos Caco-2 e o fenótipo das células M. O modelo foi utilizado para avaliar o transporte e a permeabilidade da curcumina livre e encapsulada sendo o transporte estabelecido nesta co-cultura como $1,0 \times 10^{-7}$ cm/s.

Palavras-chave:

Curcumina, Caco-2, PGSS®, modelo de co-cultura tripla, partículas lipídicas solidas.

List of Contents

List of Figures

List of Tables

List of Abbreviations

Abbreviation	Full form
%C	Curcumin load
Caco-2	Caco-2 human colorectal adenocarcinoma cell line
CCFC	Central Composite Face-Centered cube design
DLS	Dynamic light scattering
DMEM	Dulbecco's Modified Eagle's Medium
DSC	Differential Scanning Calorimetry
EE	Encapsulation efficiency
FBS	Fetal Bovine Serum
FFA	Free fat acids
GI	Gastrointestinal
HBSS	Hanks Balanced Salt Solution
HPLC	High-performance liquid chromatography
IVD	*In vitro* digestion
LCT	Low chain triglycerides
LD	Laser diffraction
M cells	Microfold cells
MCT	Medium chain triglycerides
MEM-NEAA	Non exencial aminoacids
M-like cells	Microfold-like cells
MTS	CellTiter 96® AQueous One Solution Cell Proliferation Assay reagent
MTX	Methotrexate
NE-LCT	MCT Based nanoemulsions
NE-MCT	MCT Based nanoemulsions
O/W	Oil in Water
P	Pressure
P_{app}	Apparent permeability coefficient

PBS	Phosphate Buffer Solution
PDI	Particles dispersion index
P-gp	P-glycoprotein
PGSS®	Particles from Gas Saturated Solutions
PPs	Peyer's Patches
PS	Particle size
PST	Penicillin-Streptomycin
R^2	Correlation coefficient
R_{adj}^2	Adjusted correlation coefficient
RSM	Response Surface Methodology
$ScCO_2$	Super critical carbon dioxide
SD	Standard deviation
SEM	Scanning electron microscopy
SFE	Supercritical fluid extraction
SGF	Simulated gastric fluid
SIF	Simulated intestinal fluid
SLM	Solid lipid microparticles
SLP	Solid lipid particles
SSF	Simulated salivary fluid
T	Temperature
TEER	Transepithelial electrical resistance
TP	Triple point
UV	Ultra-Violet

1. Introduction

1.1. Food industry – Functional foods and Nutraceuticals

Nowadays, the world population are understandably more interested in the potential benefits of nutritional support for disease control or prevention and tends to eat more nutritional foods.[1] These diets are known to have a lower incidence of cardiovascular diseases and certain types of cancer. With the increase of this concern and through epidemiological and clinical studies an evident relationship between diet and health is observed. [1,2] In the past few years, many food bioactive constituents, functional ingredients (vitamins, antimicrobials, antioxidants, colorants, etc.), have been commercialized in form food supplements that incorporate food extracts to obtain a product with a beneficial physiological function attributed.[3] With these modifications these resulting products cannot be classified as 'food' and in in 1989 the term ''nutraceutical'' was formed by the Foundation for Innovation in Medicine (New York, US). A new hybrid term that represents both nutrients and pharmaceuticals to designate the new foods created. The term ''functional food'' are known by the Institute of Medicine of the National Academy of Sciences (1994) as any food or food ingredient that, when consumed regularly, may provide a health benefit beyond their nutritional properties.[4]

The concepts of nutraceuticals, functional foods, or dietary supplements are confusing and most often they can be used interchangeably. Dietary supplements which, through a bioactive agent, are presented as a non-food matrix and used with the function of improving health through dosages that exceed those that could be obtained from of normal food.[2,3,5,6]

The aim of nutraceuticals is significantly different from functional food, with emphasis on prevention and treatment of diseases. Various nutraceuticals are used in nutritional therapy, which is mainly based on scientific research and with more clear information about chemical structures, biological functions and clinical information.[7] Therefore, these characteristics attracted the attention of people to seek a better diet and the production of new functional foods meeting the needs of growing Human population.

1.1.1. Bioactive Compounds

Across cultures there are many different dietary patterns, some of which promote health and others that increase risk of chronic disease. Despite cultural differences there are some shared characteristics of healthy dietary patterns. These compounds are extra nutritional constituents that typically occur in small quantities in foods. [3]

1.1.1.1. Curcumin as a nutraceutical

Curcumin [(E,E)-1,7-bis(4-hydroxy-3-methoxy-phenyl)-1,6-heptadiene-3,5-ione] (Figure 1.1), a hydrophobic polyphenol, is the main phenolic pigment extracted from turmeric, the powdered rhizome of *Curcuma longa* (Figure 1.2), widely cultivated in several tropical areas in Asia and despite the use in medicine, cosmetics and pharmaceutical preparations is mainly utilized as spice.[8–12]

The medicinal importance of powdered coloured extracts of dried roots, often called turmeric, is well documented. It has been used for many diets in particularly as an anti-inflammatory agent, however curcumin, identified as the active principle, has been shown to exhibit antioxidant, antimicrobial, anti-inflammatory, anticarcinogenic activities, etc. [8,13–15]

Curcumin and turmeric products have been characterized as safe by health authorities such as the Food and Drug Administration in United States of America, the Natural Health Products Directorate of Canada, and the Expert Joint Commit- tee of the Food and Agriculture Organization/World Health Organization on food additives.[11] While in EU it bears a status of food ingredient (E100) and is present in many food additives. [16,17]

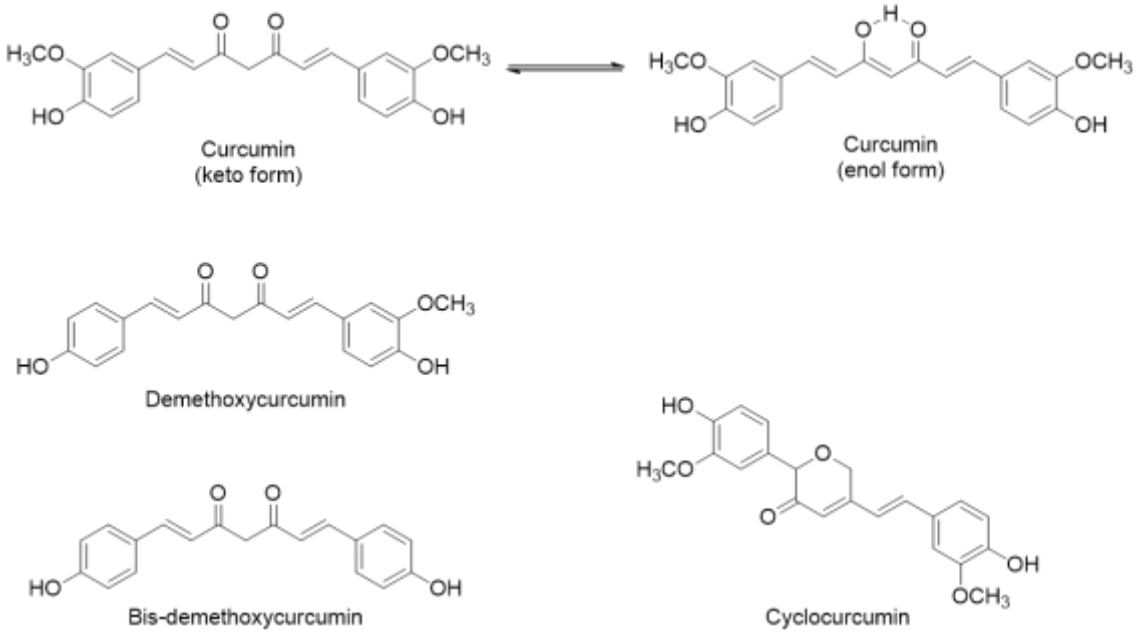

Figure 1.1| Chemical structures of curcuminoids. Adapted from Shiyou Li et al. [19]

The turmeric contains three principal curcuminoids: 75-80% curcumin, 15-20% demethoxycurcumin, 3-5% bis-demethoxycurcumin. In recent studies cyclocurcumin appears as the fourth most abundant curcuminoid in turmeric (Figure 1.3). [18–20] Curcumin, first isolated in 1815, is found as a crystalline powder insoluble in water under acidic or neutral conditions but soluble in ethanol, alkali, ketone, acetic acid and chloroform. Is unstable undergoing rapid hydrolytic degradation in neutral or alkaline conditions to feruloyl methane and ferulic acid. Since it is insoluble in aqueous medium and has poor stability towards light, alkalinity, enzymes and heat, it cannot really be widely used in food and pharmaceutical processing industry. [10,19,21]

As health promoting agent, curcumin, is limited by its poor solubility in aqueous solution and its low bioavailability. [13] Due to these limitations, studies have been developed with the aim to reduce the rapid degradation and increase curcumin's bioavailability. These studies are based on encapsulation techniques and nanotechnological approaches, however the increased bioavailability of curcumin will depend mainly on the physicochemical properties of the carrier.

1.2. Bioactives formulation

Particle formation and encapsulation technologies are widely employed in the pharmaceutical, cosmetic and food industries. However, the development of suitable delivery systems is fundamental to overcome barriers to bioactive usefulness.

Many formulations consist in comprising a core material (the active component) surrounded by a coating material (typically a bio-polymer) (Figure 1.3). The resulting materials and systems can be designed to exhibit novel and significantly improved chemical and biological properties. [22,23]

In the field of particulate delivery systems, the ability to control size, morphology and release of encapsulated compounds is fundamental to good targeting but is often held back by severe processing conditions or inadequate methods. These methods presuppose two important requirements: the encapsulation system must preserve stability of the bioactive compounds during processing and storage and to prevent undesirable interactions with food matrix, which should be depends on the type of molecule and carrier.[22,24] There is a multitude of possible ways to encapsulate bioactives. [22,23,25] Triglycerides based-nanoemulsions and supercritical fluids encapsulation techniques are the one type of formulations explored in this work.

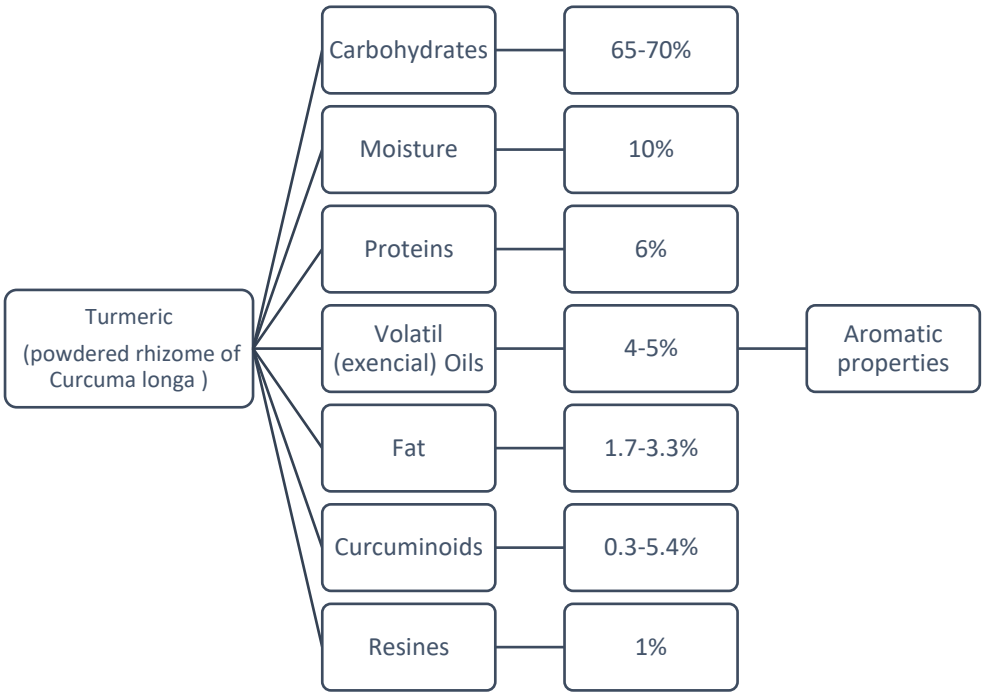

Figure 1.2| Turmeric constitution. Approximate ranges are shown based on supporting references 8, 10 and 11. The focus it's curcuminoids composition that include curcumin, demethoxycurcumin, bis-demethoxycurcumin, and cyclocurcumin.

1.2.1.Nanoemulsion-based delivery systems

Emulsions of O/W are regarded as useful tools with a great potential in the food sector to incorporate food ingredients. [26]

In general, nanoemulsions can be produced using a variety of methods within two different approaches: high energy or low energy approaches. High energy methods result from the application of high disruptive forces through mechanical devices, with the aim of causing the rupture of oil droplets dispersing them in the aqueous phase. The second approach, low energy, depends on the spontaneous formation of tiny oil droplets within mixed oil-water-emulsifier systems when changing the solution or ambient conditions, such as composition or temperature. [27–29]

The formulation of nanoemulsions consist of a mixture of immiscible liquids. Briefly, a lipid phase, that generally acts as a carrier of lipophilic active compounds, is dispersed in an aqueous phase in the form of nanometric scaled droplets (<100nm). [27] The oil phase can be constituted by different non-polar compounds, normally triglycerides are used. Besides the lipid and aqueous phases, the formulation of nanoemulsions requires the use of stabilizers such as emulsifiers to prevent the breakdown of the nanoemulsion structure. [28,30]

1.2.2.Solid lipid particles

Solid lipid particles have emerged in the last two decades as an alternative to liposomes, emulsions or polymer particles as potential release vehicles (Figure 1.3). [31] Usually comprised of biodegradable and non-toxic lipids, solid at room and body temperature, promote the release of the incorporated compound through a prolonged profile after administration at a constant concentration of the molecule of interest in the blood stream. [32,33] In addition, these vehicles have the advantage of increasing particle uptake by epithelial cells and can promote sustained drug release.

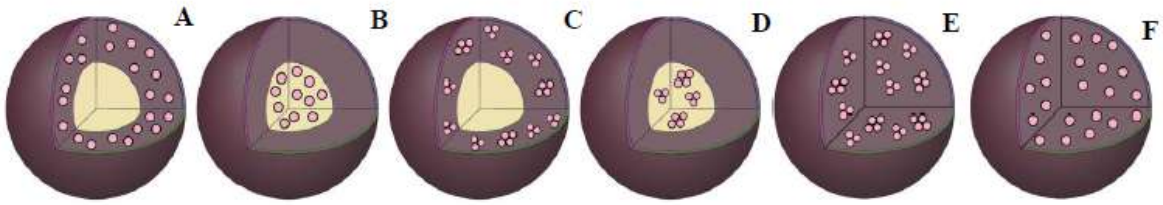

Figure 1.3| Structures of solid lipid particles according to the distribution of drug molecules (pink dots) in the lipid matrix (brown filling). The grouped pink dots symbolize drug molecules not soluble in the matrix but dispersed in other hand the dispersed ones represent drug dispersed on molecular form. (A-D) capsules; (E-F) spheres. Adapted from A. Sao Pedro. [126]

1.3. Supercritical fluid technology

Solvents are used in large amounts in the chemical, pharmaceutical, food, and natural product industries. The call for new products with singular features and design of new environmentally friendly

and sustainable technologies is emerging in society and shifting the technological processes towards high pressure. [32]

A pure component is considered to be in a supercritical state if its temperature and its pressure are higher than the critical values. The critical point represents the end of the vaporization curve in the PT phase diagram (Figure 1.4). These types of fluids add a new important property to conventional (liquid) solvents: their density; liquid-like densities and, therefore, solvating characteristics equivalents that can be easily tuned to the process needs. But, at the same time, they present gas-like properties such as very low surface tensions, low viscosities, and moderately high diffusion coefficients. In general, the physical properties in the critical region enhance mass and heat transfer processes. [34–37]

The most widely used SCF is $scCO_2$, which is nontoxic, non-flammable, cheap, widely available and easy recyclable. Once its critical properties can be achieved at moderate pressures and near-ambient temperatures (Table 1), is one of the most fluid used as “green solvent” for bioactives encapsulation. Furthermore, the use of $ScCO_2$ eliminates or reduces the use of toxic organic solvents, in the process, and allows to obtain solvent-free products due to the high solubility of most organic solvents in the fluid. [36,38,39]

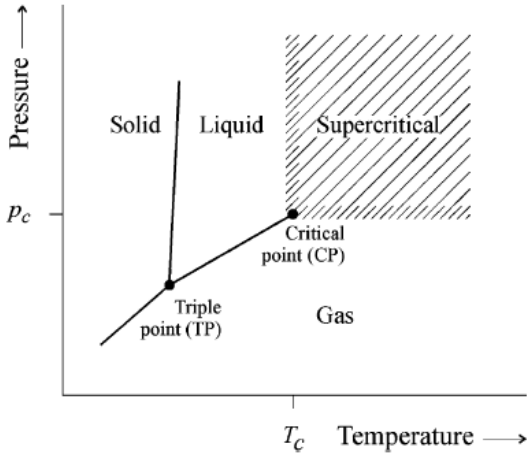

Figure 1.4| Phase diagram of a compound (PT). [37]

1.3.1.Supercritical-based precipitation methods

The use of $scCO_2$ provides several advantages in comparison with conventional techniques or even comparing with other supercritical fluids. It can be used as a solvent, antisolvent, as extracting agent or even to improve the spraying process in different techniques. The solvent properties of $scCO_2$, i.e. the solubility of polymers in $scCO_2$ and the solubility of CO_2 in the polymers, are two key fundamental subjects in this field.

The solvent power of supercritical $scCO_2$ can be used to dissolves non-polar or slightly polar compounds and decreases with the increase of compounds molecular weight. Has high affinity with oxygenated organic compounds and exhibit low solubilities for free fatty acids, glycerides and water (<0.5 wt%), at temperatures below 100 °C. One of the most interesting characteristic is the capability to

separate compound that are less volatile, have a higher molecular weight and/or are more polar, as pressure increases. However, proteins, polysaccharides, sugars and mineral salts are insoluble. [34,36,37]

1.3.1.1. Particles from Gas Saturated Solutions

The PGSS® technique was patented by Weidner et al [40–42] and allows to form particles from substances that are non-soluble in supercritical fluid. Briefly, compounds mixture absorb a large amount of CO_2 that cause a decrease of melting point (glass transition temperature for amorphous polymers) or a swelling effect on the substance.[40,43,44] The major advantages of this process, in comparison with other supercritical-based precipitation methods, is the low intake of carbon dioxide and the possibility to process thermolabile substances.

The polymeric or lipidic solution formed, which can contain between 5-50 wt% of the compressed gas, is expanded through a nozzle causing the release of CO_2 with large cooling effect, due to the energy consumption, leading to a quasi-instantaneous solidification of the droplets. This rapid cooling of the gas during the expansion process is due to the Joule-Thomson effect. In few words, since an expansion of a gas from high to low pressure through a throttle valve is an isenthalpic process, it leads to a significant temperature drop. [45–47]

The morphology, size and apparent density of the produced particles may depend on several parameters such as the structure and viscosity of the compounds to be precipitated, the operating conditions, and even the equipment used to perform the PGSS® process. [36,44,48,49]

1.4. Concepts and models for bioactives permeability studies

Prediction of human intestinal absorption, bioavailability and compounds cytotoxicity is a major goal in the optimization and production of drugs and formulated products intended for non-invasive delivery. Oral bioavailability is a highly desirable property for molecules of particulate interest nonetheless poor permeability and/or absorption make a molecule unsuitable for further development, and there is interest in finding ways to avoid the situation of having a potent, yet impermeable molecule. [50,51] The determination of oral bioavailability is as important as identifying the potential therapeutic uses of nutraceuticals. Consequently, various techniques have been currently employed to predict bioactive compounds absorption in the different phases of discovery and development. [52]

1.4.1. Bioactive compounds oral administration

Over recent years, a major challenge in compounds delivery has been the design of appropriate vehicles for the oral administration of bioactives. Bioavailability represents both the quantity of the active component absorbed through the blood circulation and the rate of this phenomenon. However, is extremely conditioned for enzymatic degradation and poor penetration of the intestinal membrane. [53] Not all concentration of the active compounds is absorbed by the epithelium being that the quantity of

drug reaching the general circulation depends on many different factors and is mostly determined by its physicochemical properties. To predict the compounds intestinal behaviour strategies for modulating tight-junction permeability increasing paracellular transport of molecules has been implemented. [54,55]

1.4.2.Intestinal composition and permeability

In oral administration absorption of compounds by passive diffusion in the intestinal epithelium (Figure 1.5) is the major transport mechanism presented. Nonetheless to be absorbed, the molecules must diffuse across a series of separate barriers. Some of them includes the mucosal side, the mucus gel layer, the intestinal epithelial cells, the lamina propria and the endothelium of the capillaries. However, only the epithelial cells barrier is the most significant to compounds absorption. [56–59] Now, several in vitro experimental models with high-throughput capacity and adequate predictability of absorption potential in human epithelial are available for evaluating intestinal permeability and transport. [60,61]

Because the oral route is the most commonly administration route used, the intestinal barrier has received much attention. In order to simulate the intestinal barrier, Caco-2 cell line have gained

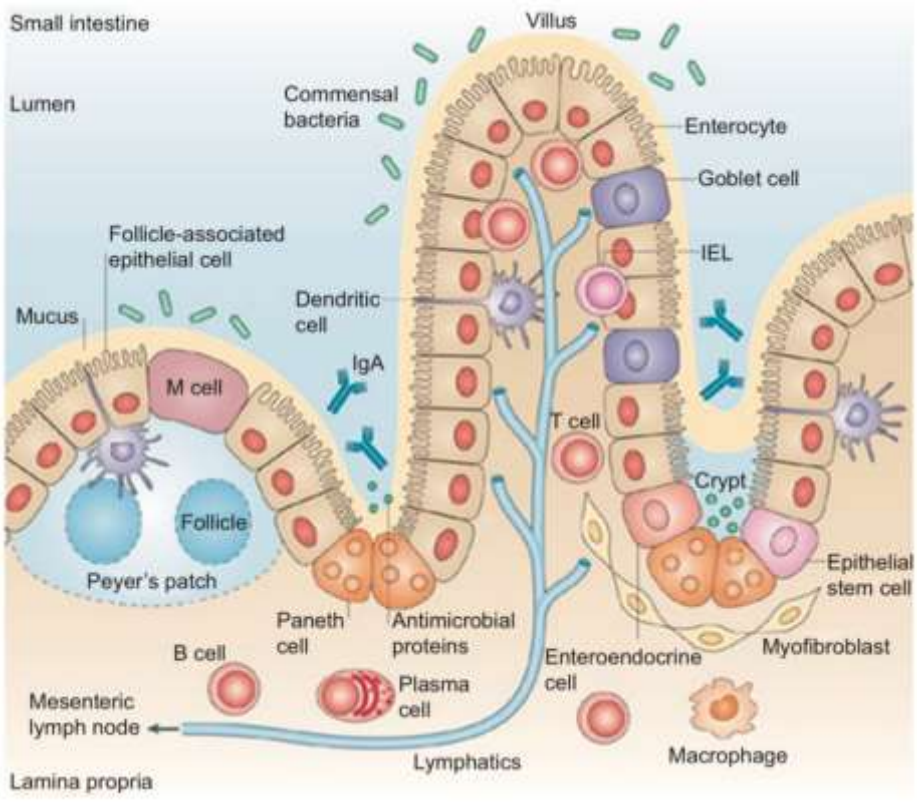

Figure 1.5| Representation of the organization of the small intestine epithelium. Adapted from Maria T. Abreu. [127]

massive approval as a reliable and high throughput *in vitro* model for evaluating a large number of candidates for their intestinal absorption potential. [55,62,63]

1.4.2.1. Caco-2 cell model

Caco-2 cells, a human colon adenocarcinoma, has been used extensively for the high throughput screening of compounds permeability. Allows effective in vitro prediction of compound permeability and absorption while considering all the physical, chemical, and biological events during intestinal transportation. [64]

They undergo spontaneous enterocytic differentiation in culture and when they reach confluency, on a semipermeable porous filter, express many primary-like qualities of enterocytes, both functional and morphological, and can fully polarize into differentiated monolayers displaying brush border regions (microvilli) and cell-cell (tight junctions).[65–68] Still, this system presents some limitations when compared to the human intestinal epithelium, specifically the overexpression of P-gp, an efflux pump, and the formation of strong tight junctions that could lead to a decrease in the paracellular permeability. Nevertheless, these monocultures only characterize absorptive cells, which do not mimic completely the human intestinal epithelium as it is a combination of different cell types: absorptive cells or enterocytes, goblet cells (mucus producer cells), endocrine cells and M cells. Being the enterocytes the most abundant cells, followed by goblet cells. [55,69–71]

Studies regarding membrane transport are still present as inconsistent due to the high requirement on the quality of the monolayer. Factors such as cell condition, passage number, length of cultivation and circumstance under which the study is performed diverge among laboratories and affects the viability of the results. [65]

1.4.2.2. M Cells

In the intestine, PPs are the major sites of antigen and microorganism sampling. M cells (Figure 1.6) are responsible for the transepithelial transport of foreign material and microorganisms from the external environment to the lymphoid follicles. [72,73] These cells typically contain a small number of microvilli in the apical zone and a basolateral cytoplasmic invagination in which the lymphocytes and macrophages are located. Passage of antigens and microorganisms through M cells is an essential step for the development of mucosal immune responses and the pathology of many infectious diseases. Particle delivery vehicles are largely prevented from passing between epithelial cells by tight junctions. However, since M cells have a relatively high transcytotic capacity compared to enterocytes, can represent an efficient route for the transport of nutraceuticals carried by particulate carriers through the intestinal epithelial barrier. Kernéis et al.[74] constructed the first intestinal in vitro co-culture model based on Caco-2 cells and mouse Peyer's patch lymphocytes. The interaction of the epithelial cell line Caco-2 with lymphocytes triggered the formation of cells-like M cells that resemble intestinal M cells functions and morphology. [75] Later, to overcome the use of primary murine lymphocytes, Gullberg et al. [75] developed a similar model based on a co-culture of Caco-2 cells and human Raji B lymphocytes, a cell line that is originated from a human Burkitt's linfoma, since Raji cells exhibit B cell markers, which are major inductive of M cells phenotype. [76] Results based on the work of des Rieux et al. [54,77] exhibited that particle transport through the M cell model was 50-fold higher compared to a pure Caco-2 monolayer.

Like described for Antunes et al. [60] to obtain the phenotype M-cell like, one common approach is to use a 21 days in vitro model that consists in a co-culture of Caco-2 cells seeded on Transwell® membranes inserts (normal oriented) (Figure 1.7) and human Raji B lymphocytes added, to the basolateral chamber of the insert, after 14 days. Whit this method it was possible to detect that some cells developed M-cell like morphology.

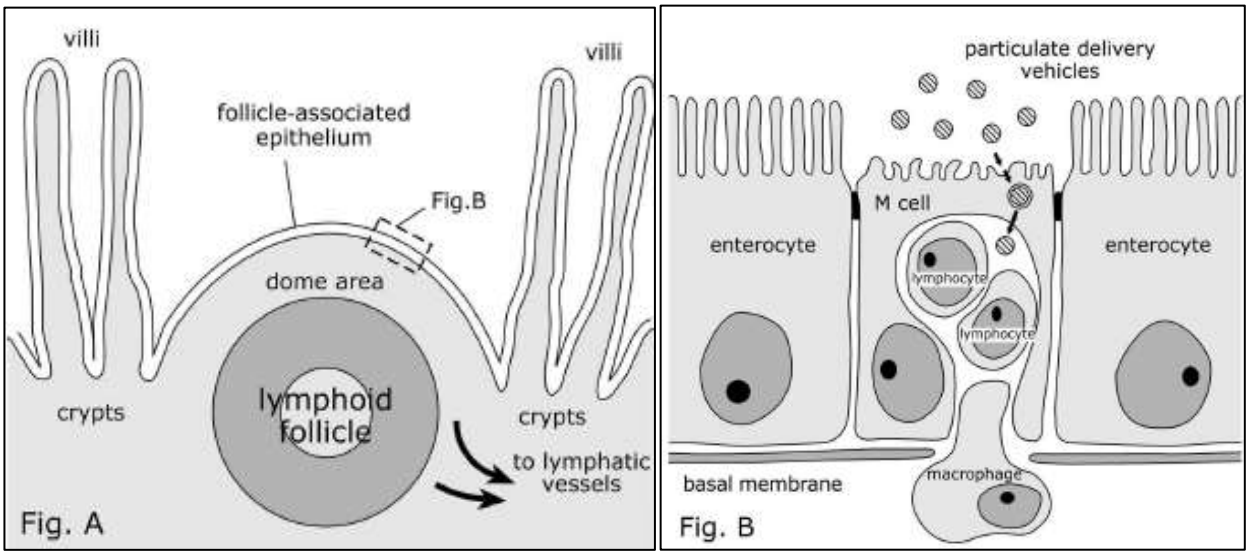

Figure 1.6| Schematic sections of Peyer's lymphoid follicle and follicle-associated epithelium (FAE), showing the transport of particulate delivery vehicles by M cells. The lymphoid follicle is situated under the projecting area in the intestinal lumen between the villi. Covered by FAE, this epithelium is characterized by the presence of specialized antigen-sampling M cells (Fig. B). Adapted from Clark et al, 2001. [72]

1.4.2.3. Caco-2/HT29-MTX/Raji B Model

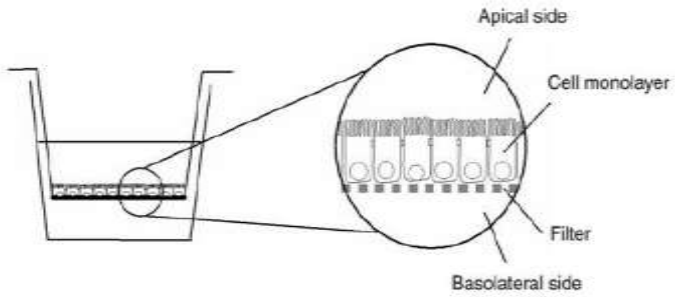

Figure 1.7| Schematic representation of a Transwell® co-culture model. Caco-2/HT29-MTX cells are seeded on the polycarbonate inserts at the apical side while Raji B are added later to the basolateral compartment. Image adapted from Hubatsch et al, 2007.[128]

The mucus layer covering GI tract, represents a significant barrier to particles absorption. Mucus is a viscoelastic adhesive gel that coats all exposed epithelial surfaces not covered by skin.[78] Mucus protects the underlying epithelium by both lubricating the surface and trapping and removing foreign particulates. Has been shown to be highly adhesive to pathogens and particulate systems, offering many opportunities for the development of adhesive interactions with small polymeric particles. [79,80]

Since the early 1980s, several methods have been developed to differentiate the adenocarcinoma cell line HT29 into mature intestinal cells under appropriate culturing conditions. [81] Through selective pressure with MTX a distinct subpopulation of mucus-secreting HT29 cells that maintain their ability to differentiate under normal culture conditions were isolated by Lesuffleur et al. [82] At late confluence, HT29-MTX monolayers show a dense mucus layer on their apical surface and a morphology identical to human intestinal goblet cells. However, as opposed to Caco-2 cells, does not express P-gp and do not form TJs as tight which promotes the increase in paracellular transport pathways. These mucus layers is labile and could be removed by extensive and rough washings. [81,83,84]

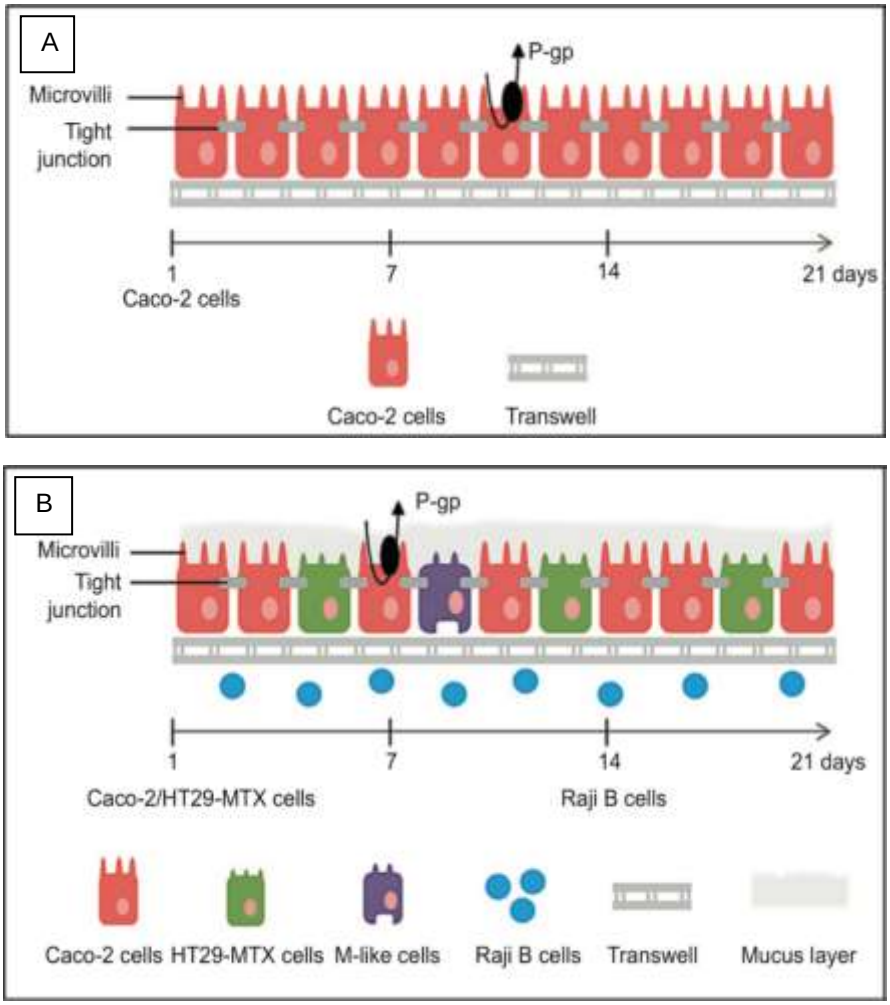

Figure 1.8| Illustration of A) Caco-2 monolayer and B) Caco-2/HT29-MTX/Raji B co-culture model setup. Adapted from C.Pereira et al.[52]

Considering the above-mentioned culture models all their advantages and drawbacks, a cell-based model based on the combination of Caco-2, mucus-producing HT29 cells and Raji B lymphocytes was stablished resulting in a more promising experimental results reproducing the intestinal epithelium in a more complete way like illustrated in figure 8. [55,61]

1.5. Aim and rational of the thesis

The challenge addressed in this work was using an *in vitro* cell co-culture model that mimics the intestinal epithelium to evaluate the bioavailability and safety of curcumin delivery systems.

To achieve this goal, an integrated approach was developed by two distinct tasks:

1. Development of different types of curcumin formulations to maximize its bioavailability and stability.
2. Implementation of an in vitro model system that closely mimics the human intestinal epithelium monolayer to evaluate the formulated curcumin systems in terms of toxicity and bioavailability.

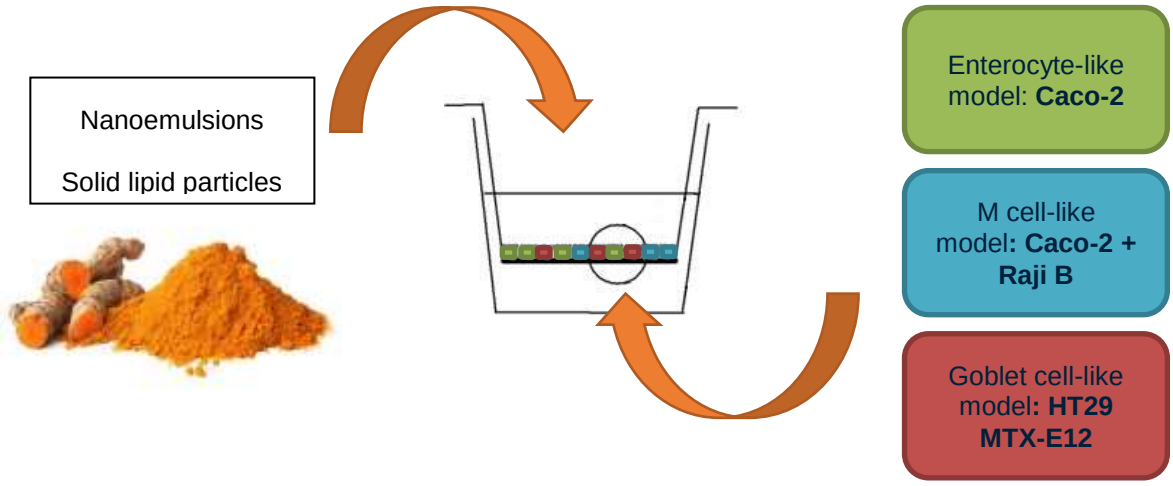

In task 1: Curcumin delivery systems

The general aim of this first task was the investigation of curcumin entrapment into solid lipid microparticles, using a green technology, on assisted CO_2 precipitation method and compare this formulation whit particles prepared by conventional approaches. The PGSS® process was chosen and a response surface methodology was used to model and optimize the encapsulation conditions.

Different techniques were applied to characterize the formulations in terms of morphology, size and thermal behaviour along with the quantification of encapsulated curcumin. After total characterization these particles underwent an in vitro digestion process used to evaluate the changes in curcumin formulations throughout the gastrointestinal tract.

In task 2: In vitro cell co-culture model

A triple co-culture has been established and characterized for use as an in vitro tool for transport and permeability studies. Viability and cytotoxicity profiles tests of free and encapsulated curcumin were evaluated for different dosages and times of exposure. The integrity of the monolayer and the quality of tight junctions were controlled during the transport studies by monitoring transepithelial electrical

resistance and by microscopic observation of cell morphology. The amounts of permeated curcumin were quantified, and apparent permeability coefficients were determined.

2. Materials

For curcumin encapsulation through PGSS® technique, curcumin (95%) was purchased from Alfa Aesar (Karlsruhe, Germany), beeswax from QUIMIND (Portugal), CO2 (99.95 and 99.998 mol% purity) was delivered by Air Liquide (Portugal) and methanol absolute 99.99% from Fisher Scientific (Waltham, MA, USA). Curcumin (65%) encapsulated in nanoformulations was purchased from Sigma-Aldrich. An analysis and comparison of its purity is shown in attachment.

To perform the *In vitro* digestion, digestion fluids were produced: SSF (KCl, 15.09 mM; KH2PO4, 1.35 mM; NaHCO3, 13.68 mM; MgCl2(H2O)6, 0.15 mM; NH4(CO3)2, 0.06 mM; CaCl2(H2O)2, 1.5 mM; HCl, 1.1 mM; pH 7), SGF (KCl, 6.9 mM; KH2PO4, 0.9 mM; NaHCO3, 25 mM; NaCl, 47.2 mM; MgCl2(H2O)6, 0.12 mM; NH4(CO3)2, 0.5 mM; CaCl2(H2O)2, 0.15 mM; HCl, 15.6 mM; pH 3) and SIF (KCl, 6.8 mM; KH2PO4, 0.8 mM; $NaHCO_3$, 85 mM; NaCl, 38.4 mM; $MgCl_2(H_2O)_6$, 0.33 mM; $CaCl_2(H_2O)_2$, 0.6 mM; HCl, 8.4 mM; pH 7). Still in the digestion procedure the following enzymes were used: α-Amylase (A1031-1KU, Sigma, USA), pepsin (EC 3.4.23.1) from porcine gastric mucosa (Sigma, USA), bile extract porcine (Sigma, USA) and porcine pancreas (Sigma-Aldrich, USA). To stop enzymatic action Pefabloc®) from Sigma-Aldrich and Amicon® Ultra-4 Centrifugal Filter Units from Merck (Millipore, Germany) was used.

All cell culture media and supplements, namely FBS, DMEM, MEM NEAA, PS, trypsin/EDTA and HBSS were obtained from Invitrogen (Gibco, Invitrogen Corporation, Paisley, UK). Corning® Transwell® polyester membrane cell culture inserts (12 mm with 0.4 µm pore polyester membrane insert and 1.12 cm^2) were purchased from Merck (CLS3460-48EA) to monolayer culture.

To perform cells cytotoxicity assays, MTS (G3582) from Promega was used and in assays with necessary cellular lysis the utilized reagents were: inhibitor of Proteases cocktail (Protease inhibitor cocktail set III ANIM #535140-1 Calbiochem) and Cell Lytic (M Cell Lysis reagent, Sigma C2978-50 ml).

Whenever it was necessary to perform sterility tests were performed on tryptone soy broth (TSB, Scharlau, Spain).

3. Methods

3.1. Curcumin formulation process

3.1.1. Curcumin Nanoformulations

3.1.1.1. Nanoemulsions preparation

Curcumin nanoemulsions were prepared through high pressure homogenization according to other authors (Pinheiro et al., 2016). The lipid phase constituted by MCT or LCT and 0.1 % of curcumin was homogenized with the aqueous phase (with lecithin 2.5 %) at room temperature and a volume ratio of 1:9. First, both solutions were pre-mixed using an Ultra-Turrax homogenizer (T 25, Ika-Werke, Germany) during 2 min and thereafter the resulting emulsion were passed through a high-pressure homogenizer (NanoDeBee, Bee International, South Easton, Massachusetts, USA) at 20 000 psi (137.9 MPa) during 20 cycles. The nanoemulsion were kept at 4 ˚C in the dark.

3.1.1.2. Solid lipid nanoparticles preparation

SLN were prepared according with Kheradmandnia et al.[85]. Beeswax (3 %), lecithin (1.5 %) and curcumin (0.1 %) were melted in a water bath at 85 ˚C. Tween 80 (1.5 %) was solubilized in distilled water at 85 ˚C in an Ultra-Turrax homogenizer (T 25, Ika-Werke, Germany) during 2 min at 3400 rpm. The aqueous solution was added to the lipid solution and mixed in an Ultra-Turrax homogenizer (T25, Ika-Werke, Germany) at 22000 rpm during 10 min. Then the resulting nanoemulsion was gradually dispersed at a volume ratio of 1:10 in cold water at 2 ˚C under stirring at 2000 rpm. The SLN were kept at 4 ˚C in the dark.

Both formulations at the nanoscale were developed and prepared out by Universidade do Minho (Portugal) within the framework of the NanoMaxiSafe project (PTDC / AGRTEC / 5215/2014), in which some of the results produced in this master thesis are also included.

3.1.2. Curcumin microparticles

3.1.2.1. Melting point measurements

The melting point of solids can be considerably decreased by using supercritical fluids which are highly soluble in the melt. Knowledge of the solid-liquid transitions of lipids under pressurized CO_2 is essential for their precipitation through the PGSS® process. Since beeswax data of melting point depression, as a result of CO_2 dissolution in the matrix, is not a topic presented in the literature the melting point depression was measured within this work using a visual method. [86,87]

For performing the melting point determination experiments, a stainless steel high-pressure visual cell with an internal volume of approximately 5 cm^3 with two sapphire windows was used. Briefly, the lipid was placed inside a glass (1 cm^3) and inserted in the visual cell. The pressure in the cell was

measured with a pressure transducer Digibar II calibrated between 0 and 250 bar (accuracy: 0.15 %) and the CO_2 was pumped, using a Haskel pump (model 29723-71), until the desired pressure was reached. The temperature was then gradually increased until it was possible to visually observe the complete melting of the lipid. The heating system was composed of a heating cable (Horst), a controller (Ero Electronic LMS) and a high accuracy thermometer (Omega HH 501 AT, 0.1 %). Measurements were performed in a pressure range up to 200 bar. To confirm the reproducibility of the results some points were repeated resulting in a 0.15 % of error.

3.1.2.2. Particles from gas saturated solutions

Beeswax particles unloaded and loaded with 10 wt % of curcumin were produced by PGSS® in batch mode. The schematic representation of the modified PGSS® equipment (FAME UNIT, Separex, France) used to produce the particles is shown in figure 3.1 previously described in the work of Rodríguez-Rojo et al. with some modifications. [88] Briefly, CO_2 was fed by a pneumatic pump (29723-71, Haskel International Inc.,CA, USA) to a 50 cm^3 high pressure stirred vessel, electrically thermostated, at the selected operation temperature until the desired working pressure was reached. Then, the stirred mixture is depressurized through a nozzle (250 µm) by an automated depressurization valve to a cyclone, where it was externally mixed with compressed air (7 bar). The mixture and the supercritical carbon dioxide are brought into contact during 15 min. Finally, the particles were recovered into a collector vessel of 18 L at atmospheric pressure. The operating conditions (T and P) were chosen according to the measurements of melting point depression of the lipid in the presence of compressed CO_2 and varied to see their effect on the particles' morphology and size.

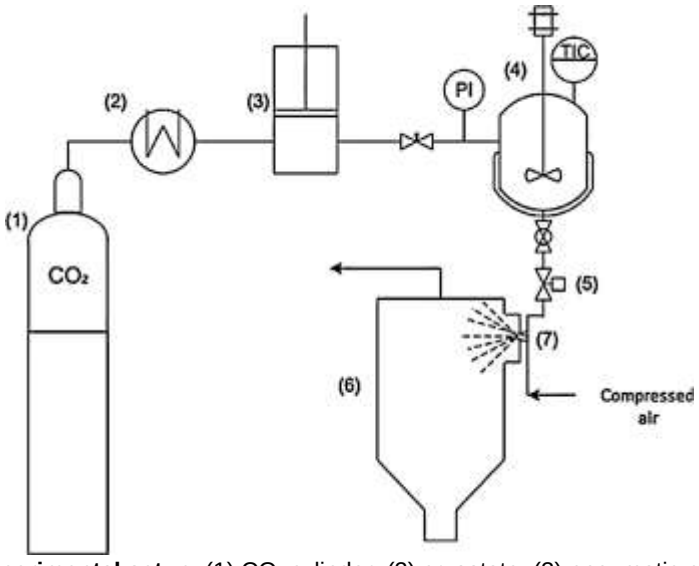

Figure 3.1| PGSS® experimental setup: (1) CO_2 cylinder, (2) cryostate, (3) pneumatic piston pump, (4) stirred vessel (electrically thermostated), (5) automated depressurization valve, (6) recovery vessel, (7) nozzle. Adapted from V.S.S. Gonçalves et al. [89]

3.1.2.3. Experimental design (Process Optimization)

RSM was used to model and optimize encapsulation conditions. RSM consists of a set of mathematical and statistical methods developed for modelling phenomena and finding combinations of several experimental factors (variables) that will lead to optimum responses. With RSM, several variables are tested simultaneously with a minimum number of trials, using special experimental designs that enable to find interactions between the variables which cannot be identified with classical approaches. The encapsulation of curcumin through PGSS® was carried out following a CCFC, as a function of three factors: pressure, temperature and curcumin load in mixture. The design consisted of seventeen randomized runs with three replicates at the central point described in table 3.1. To normalize parameters, each of the coded variables was forced to range from -1 to 1, so that they all affect the response more evenly (Table 3.2). The repetitions of the centre points are used to determine the experimental error, which is assumed to be constant along the experimental domains. The fit of the models was evaluated by the R^2 and R_{adj}^2.

Table 3.1| Three-factor, three-level face-centered cube design used for RSM.

		Independent variables		
Standard[1] Order	**Run[2] Order**	**Pressure (bar)**	**Temperature (ºC)**	**Curcumin load (%)**
1	5	80 (-1)	63 (-1)	1 (-1)
2	2	160 (1)	63 (-1)	1 (-1)
3	1	80 (-1)	73 (1)	1 (-1)
4	7	160 (1)	73 (1)	1 (-1)
5	8	80 (-1)	63 (-1)	10 (1)
6	11	160 (1)	63 (-1)	10 (1)
7	4	80 (-1)	73 (1)	10 (1)
8	15	160 (1)	73 (1)	10 (1)
9	9	80 (-1)	68 (0)	5.5 (0)
10	16	160 (1)	68 (0)	5.5 (0)
11	13	120 (0)	63 (-1)	5.5 (0)
12	12	120 (0)	73 (1)	5.5 (0)
13	17	120 (0)	68 (0)	1 (-1)
14	6	120 (0)	68 (0)	10 (1)
15	3	120 (0)	68 (0)	5.5 (0)
16	10	120 (0)	68 (0)	5.5 (0)
17	14	120 (0)	68 (0)	5.5 (0)

[1] No randomized

[2] Randomized

Table 3.2| Real values of the variables for the coded ones.

Independent variable	Factor levels		
	-1	0	1
Pressure (bar)	80	120	160
Temperature (ºC)	63	68	73
Curcumin load (wt %)	1	5.5	10

3.2. Particles' characterization

3.2.1.DSC measurements

DSC was performed using a TA instruments Q200 (module MDSC) with the aim of studying the thermal behaviour of the particle's components. An amount of 5-10 mg of curcumin or pure lipid (beeswax) was weighted into an aluminium pan and sealed in the calorimeter. The samples were heated from 0 °C to 220 °C at a rate of 10 °C/min under nitrogen atmosphere. After encapsulation procedure an amount of 0.4-1 mg of lipid particles were tested to in the same conditions.

3.2.2.Encapsulation efficiency

To measure the total curcumin encapsulated in PGSS produced microparticles, curcumin (an amount of 5 and 7 mg of particles) was extracted from the lipidic matrix with 30 mL of methanol in an ultrasound bath during 30 min. The result of this disruption was later analysed by a UV/Vis spectrophotometer (model EPOCH, 219 Bio-Tek, USA) wavelength of 420 nm. To eliminate non-dissolved solids before the quantification the solution was filtered (25 mm - 0.20 µm).

The determined absorbance is proportional to the amount of curcumin in solution. The amount of curcumin in the solution is reported in this work as the percentage of encapsulated curcumin. Standard solutions of curcumin to be used in the calibration was obtained by using standard samples in methanol with concentrations between 1 and 25 µg/mL (R^2 =0.9992). For reproducibility purposes average and standard deviation were calculated from 3-4 replicates. On the other hand, the encapsulation efficiency (Eq. 1) was obtained comparing the final and initial load of curcumin in the experiment.

$$EE\ (\%) = \frac{Final\ curcumin\ load}{Inicial\ curcumin\ amount} \times 100\ (\mathbf{Eq.\ 1})$$

3.2.3.Particle size and morphology

The morphology of the particles was analyzed and imaged by SEM (Jeol, JSM-5310 model, Japan). Samples were prepared for observation by covering with gold/palladium (Au/Pd), approximately 300 ˚A of gold, in a sputter coater (Quorum Technologies, model Q150TES). Micrographs of the prepared aliquots were taken at an acceleration voltage of 20 kV.

The particle size of the samples was measured by a LD equipment model Malvern Mastersizer 2000. The particle size measurements are defined as d0.5 (known as the median particle size by volume) being the result the average from 3 measurements. The span value is also reported, that is, the ratio between d0.5 and (d0.9-d0.1); span values near to 1 represent narrow PDI.

3.2.4.Curcumin formulations sterilization

Briefly, microparticles were put directly in contact with UV irradiation during 30 min at room temperature in laminar flux chamber and to further confirm sterility, microparticles were incubated in tryptone soya broth at 37 °C in a humidified atmosphere of 5 % CO_2 to ensure the absence of bacterial contamination (data not shown).

3.3. *In Vitro* Release of Curcumin

The in vitro curcumin release assays were performed in two different environments: simulated intestinal fluid and simulated gastric fluid, both without the presence of enzymes. This test had three different approaches: solubility in SIF, SGF and SIF plus SGF. For each fluid 5 mg of PGSS microparticles were deposited in a sealed flask with 30 ml of SIF or SGF. The system was kept under constant agitation (50 rpm) at 37 °C during 48 h. In the last-mentioned approach, the compound was subjected to two hours of incubation with SGF to which a volume of SIF (1: 2 respectively) was added over the remaining assay time. At a desired time interval, an aliquot of 1 mL was removed, with replacement with fresh fluid, from each flask to quantify through UV/Vis measurements like described in 3.2.2. The aliquots were filtered (25 mm - 0.20 µm) before the UV/Vis analysis to avoid the interference of microparticles. The same procedure was repeated to free curcumin, where 1 mg of curcumin (95 %) was submitted to 40 mL of digestion fluids.

3.4. *In vitro* Digestion

An *in vitro* digestion procedure, as described by Minekus et al. [90] was used to evaluate the transformation that encapsulated curcumin suffer throughout the gastrointestinal tract. These methods try to mimic physiological conditions in vivo, considering the presence of digestive enzymes and their concentrations, pH, digestion time, and salt concentrations, among other factors, to mimic closely the oral, gastric an intestinal phase property.

3.4.1.Oral Phase

First, the oral phase, 5 mL of microparticles were added to 4 mL of Simulated Salivary Fluid. Since microparticles are in solid state 0.5 mL α-Amylase (150 U/mL in fluid) were required. To adjust the pH to 7 was add 6 M NaOH and Milli-Q water to a final volume of 10 mL. The mixture was incubated for 2 minutes at 37°C, under constant agitation.

3.4.2.Gastric Phase

The mixture resulting from the oral phase was submitted to a gastric phase by adding 8 mL of Simulated Gastric Fluid and 1 mL of pepsin (2000 U/mL in fluid) from porcine gastric mucosa. In this phase, 1M HCl was added until pH 3 was stablished and Milli-Q water to perform a final volume of 20 mL. The gastric digestion step was conducted for 2 hours at 37°C, under constant agitation.

3.4.3.Small Intestine Phase

To the gastric digestion mixture were added 11 mL of Simulated Intestinal Fluid, 2.5 mL of bile extract porcine and 5 mL pancreatin from porcine pancreas (200 U/mL in the fluid). Finally, the mixture was brought to pH 7 by addition of 6 M NaOH and Milli-Q water added to a final volume of 40 mL. Like gastric phase incubation of intestinal digestion mixture occurred for 2 hours at 37 °C, under constant agitation.

To stop enzymatic action on the intestinal digestion sample proceeded the addition of 10 µL of Pefabloc® per millilitre of digested sample. The mixture was transferred to Amicon® Filter and centrifuged (Mikro 220R, Hettich, Germany) at the maximal velocity, normally 4000 G, for 40 minutes. All collected samples were stored at -20 °C until further use.

3.5. *In vitro* cell-based assays

3.5.1.Cell Culture and sub culturing

To determine cellular viability as used a standard trypan blue staining procedure followed by cell counting in hemocytometer. Every time complete medium or trypsin was needed, to cell culturing, were pre-warmed at 37 °C.

3.5.1.1. Adherent cells culture

The human colon adenocarcinoma Caco-2 cells, purchased from Deutsche Sammlung von Microorganismen und Zellkulturen (Braunschweig, Germany) and HT29-MTX-E12 (12040401), European Collection of Authenticated Cell Cultures, were grown in a standard medium Dulbecco's DMEM supplemented with 10 % heat-inactivated FBS, 1 % MEM NEAA and 1 % PST and maintained at 37 °C in a humidified atmosphere of 5 % CO_2. The stock cells were maintained as monolayers in 175 cm^2 culture flasks regularly sub-cultured when reaching 70-80 % of confluence with medium change every two or three days. To detach them a 0.25 % (w/v) Trypsin-EDTA solution was used for 5-7 minutes at 37 °C.

3.5.1.2. Non-adherent cells culture

Human Burkitt's lymphoma Raji B (85011429) from European Collection of Authenticated Cell Cultures were grown in a standard DMEM medium supplemented with 10 % heat-inactivated FBS, 1 % MEM NEAA and 1 % PST and maintained at 37 °C in a humidified atmosphere of 5 % CO_2. The stock cells were maintained as monolayers in 175 cm^2 culture flasks with medium change every three days.

3.5.2.In *vitro cell* models

The techniques employed to obtain the models used for the in vitro experiments were described in Araújo et al. paper [55]. Monocultures of Caco-2 cells and a triple co-culture of Caco-2:HT29-MTX-E12:Raji B with a proportion of 90:10 between Caco-2 and HT29-MTX-E12 cells, respectively, to reach a monolayer with a final density of $1x10^5$ cells/cm^2 were grown in the apical compartment of Transwell® inserts and were maintained for 21 days under a 5 % CO_2 humidified atmosphere at 37 °C.

Caco-2 monolayer and a co-culture of Caco-2 cells with HT29-MTX-E12 were maintained under standard incubation conditions for 14−16 days, with medium change on both, apical (0.5 mL) and basolateral sides (1.5 mL) every other day. To reach the triple culture model, $1×10^6$ Raji B cells were added to the basolateral compartment, after the co-culture grew for 16 days, and maintained during 21 days of culture. [62,91] Until the day of the experiment the basolateral medium, containing the non-adherent cells, was never changed.

3.5.2.1. Cytotoxicity assay - MTS

Toxicity assays were performed using completely differentiated Caco-2 cells. When cultured in special conditions, suffer spontaneous differentiation expressing a morphological and functional resemblance to mature enterocytes monolayer. [66]

Cells were seeded in 96-well culture plates at a density of 2 x 10^4 cells/well, and the medium changed every 48 hours. The cells were allowed to grow for 5-7 days, until confluence and differentiation were reached. Testing samples were diluted in DMEM culture medium with 0.5 % FBS, and then added to the wells, except to the control cells which contained the solvent alone. The incubation with the different formulations was carried out for 24 hours and in a 5 % CO_2 humidified atmosphere at 37 °C. The experiments were done in triplicates with cells between passages 40 and 45. [92]

Cytotoxicity evaluation was performed by colorimetric MTS assay. This assay is based on the conversion of a tetrazolium salt into a coloured, aqueous soluble formazan product by mitochondrial activity of viable cells at 37 °C. Following the incubation period (24 h at 37 °C in a 5 % CO_2 humidified atmosphere) samples were removed, cells were rinsed with PBS and 100 µL MTS was added to each well reacting for 3 hours. The viability reagent was diluted according to the manufacturer information, 16 % v/v of MTS in cell culture media (DMEM supplemented with 0.5 % FBS). After incubation, the

quantity of formazan produced was measured in a spectrophotometer (EPOCH, 219 Bio-Tek, USA) at 490 nm and is directly proportional to the number of living cells in culture.

The results were expressed as percentage (%) of cell viability relative to the control. The plates were also examined under the microscope to assess the degree of cell survival.

3.6. Triple co-culture validation and morphology

After 21 days in culture, Transwell® membranes were washed twice in PBS, following primary fixation with 3 % (v/v) glutaraldehyde (AGAR Scientific, AGAR cientific) during 45 min at room temperature. After the incubation period the glutaraldehyde was discarded, and membranes were washed with 0.1 M sodium-cacodylate buffer, following a dehydration step through a graded series of ethanol. In this step the cells were not long in touch with the different concentrations of ethanol and a solution of 75 % (v/v) HMDS was added to culture during 10 min at room temperature. After this time, inserts were air drier and membrane were analysed and imaged by SEM (Jeol, JSM-5310 model, Japan).

Samples were prepared for observation by covering with gold/palladium (Au/Pd), approximately 300 ˚A of gold, in a sputter coater (Quorum Technologies, model Q150TES) and micrographs of the prepared membranes were taken at an acceleration voltage of 15 kV. All reagents used in this fixation protocol were purchased from Sigma-Aldrich.

3.6.1. Alcian Blue assay

Alcian Blue 8GX obtained from Sigma-Aldrich (St. Louis, USA) was used to stain mucus secretion on the surface of monolayer of HT29-MTX-E12 cells. The confluent culture was washed twice with 200 µL PBS and fixed using 10 % (v/v) paraformaldehyde (contains 4 % (w/v) formaldehyde) for 20 minutes. To remove paraformaldehyde cells were rinsed again with PBS and then stained using 100 µL alcian blue stain (1 % (w/v) alcian blue in 3 % (v/v) acetic acid/water at pH 2.5) for 15 minutes. The inserts were washed several times with PBS to remove the excess marker solution and then air-dried.

3.7. Curcumin transport assay

3.7.1. Cell monolayer integrity

With medium change (every 48 h) the TEER of Caco-2 and co-culture monolayers was measured with EVOM epithelial voltohmmeter equipped with chopstick electrodes (World Precision Instruments, Sarasota, FL, USA to monitor cellular integrity before the permeability studies. To ensure integrity and confluence of entirely differentiated monolayers only inserts with TEER value higher than 600 Ω were used for the characterization experiments. [65,91]

3.7.2.Co-culture permeation assay

Culture of Caco-2 cells and triple co-culture were cultivated on permeable supports like described in 2.6.2. [93] After 20 days in culture, Caco-2 cells express several features of the mature small intestine enterocyte. [94]

After 21 days of culture, cell medium was carefully discarded from apical and basal compartments and both compartments were washed twice with HBSS pre-warm (pH 7.4) to 37 °C. Then, HBSS solution was replaced by 500 µL of the test sample appropriately diluted in culture medium. The plate was incubated at 37 °C under a 5 % CO_2 humidified atmosphere for 24 hours. At 15, 30, 60, 120, 180, 240 minutes after initiation the incubation with test samples, 200 µL, from basolateral compartment, were collected for chromatographic analyses of curcumin. TEER was measured to monitor cells monolayers integrity after samples collection.

The amount of curcumin (µg) in each compartment was determined using curcumin as an external standard for the calibration curve (0-25 ug/mL). Dose-response curves were plotted with GraphPad Prism® (version 6.01, GraphPad Software Inc., USA) and the results were expressed as means of at least duplicates of µg/mL of curcumin ± standard deviation. P_{app} was calculated from the measurement of the flow rate of curcumin from the donor to the acceptor chambers:

$$\mathrm{P_{app}\ (cm/s)} = \frac{\mathrm{dQ}}{\mathrm{dt(A \times C_O)}} \ (\mathbf{Eq.\ 2})$$

Where dQ is the total amount of permeated curcumin (µg), A is the diffusion area (cm^2), C_0 is the initial concentration of curcumin (µg/mL) and dt is the time of experiment (s). The coefficient $\left(\frac{\mathrm{dQ}}{\mathrm{dt}}\right)$ represents the steady-state flux of curcumin across the co-culture monolayer.

Membranes were washed twice with ice-cold 0.01 M PBS (Sigma-Aldrich, USA) to stop curcumin uptake. Afterwards, cells were lysed by the addition of 1 % inhibitor of Proteases cocktail for 200 µL of Cell Lytic. The plate was stirred for 15 minutes at 500 rpm and the lysate centrifuged for 15 minutes at 20 000 xg. The supernatant was stored and analysed by chromatography to determine the amount of curcumin in cell fraction.

3.7.3.Curcumin measurements

The analyses were performed on a Dionex Ultimate 3000 HPLC, equipped with a C-18 LiChrospher® 100 RP-18 (5 µm) column, at 35 °C, and with a DAD-3000 detector. The injection volume was 20 µl and the HPLC method used was as follows:

Table 3.3| HPLC method used to curcumin quantification. Flow = 0.3mL / min.

Time (min)	**% B Eluent** (90%ACN+0.5%HCOOH+H_2O)
0.100	25
5	50
10	100
18	100
20	50
25	25

A calibration curve was prepared with standard solutions containing 0.016 to 25 µg/mL of curcumin in methanol (Sigma-Aldrich). Curcumin, demethoxycurcumin, and bisdemethoxycurcumin were quantified by comparing the peak areas with the calibration curve and results are expressed in order to curcumin concentration. [18]

4. Results and discussion

4.1. Curcumin formulations

4.1.1. Particles from gas saturated solutions

4.1.1.1. Melting point measurements

Beeswax is a natural raw material used in pharmaceutical and cosmetics, suitable for food use (E-901) and other industries. It is highly crystalline and is frequently used in the preparation of controlled release drug preparations. [95] The one used in this work was obtained by melting the walls of honeycombs produced by *Apis mellifera L* bees with hot water and removal of foreign matter resulting in blocks or granules of non-crystalline structure, of yellowish colour, with a pleasant aroma of honey.

The melting point of solid substances can be depressed considerably by using supercritical fluids that are highly dissolvable in the molten substance. This fact can be used in micronization processes where thermo-labile materials are liquefied at a temperature lower than their normal. [86] A quantitative, predictive knowledge of the polymer melting point as a function of process conditions could support in the selection of materials and operating conditions for processes involving compressed fluids. [96]

The melting point depression of Beeswax under compressed CO_2 was studied in this work and the experimental data for solid-liquid transition of the lipid are presented in Figure 4.1.

The system Beeswax/CO_2 showed an initial melting point depression as the pressure increased due to the incorporation of CO_2 into the lipid matrix. The maximum reduction was 6.5 °C and was reached at a pressure of 141 bar. Above this range, the hydrostatic pressure takes place and leads to an increase in melting temperature. The same general behaviour has been observed with many substances. [45–47,86] However the melting point reduction depends on lipid characteristics.

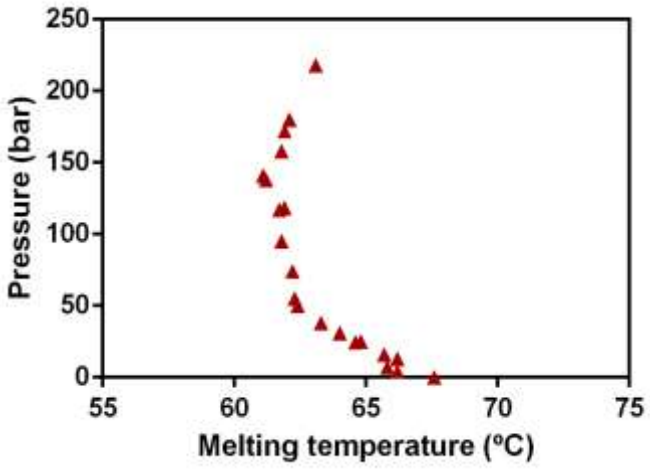

Figure 4.1| Melting points of Beeswax in the presence of CO_2.

4.1.1.2. Modelling of curcumin precipitation through PGSS®

In this study, three factors with three level CCFC design was employed to optimize curcumin entrapment process variables (temperature (T, 63-73 ºC), pressure (P, 80-160 bar) and curcumin amount (C%, 1-10 (w/w))) and to study the effect of process variables on the particle size, encapsulation efficiency and span value. A total number of 17 experiments including three center points (used to determine the experimental error) were carried out to find out the optimal process conditions (Figure 4.2). The various combinations of experimental conditions (coded and uncoded) with their respective experimental responses (mean response data) are presented in Table 4. All parameters to be used were chosen according to the melting point depression in the presence of CO_2 to ensure the liquid state of the lipids prior to atomization of the mixture. The obtained modelling results, i.e. encapsulation efficiency, particle size and span are shown in table 4.1 and were used to estimate both, linear and quadratic effects of the variables and their linear interactions.

Figure 4.2| Curcumin solid lipid particles produced by PGSS® whit different curcumin load. A) 1% Curcumin; B) 5,5% Curcumin; C) 10% Curcumin.

For span a lack of fit of the polynomial models exhibited by low values of R^2 and R_{adj}^2 was observed. The response surfaces (Figure 4.3) fitted to EE and PS can be described by second-order polynomial models as a function of curcumin load, pressure and temperature (Table 4.2). In these response surface models, the significant effects ($p<0.05$) and those having confidence range smaller than the value of the effect, or smaller than the standard deviation (data not shown), were included in the model equations of these surfaces to avoid missing an important factor. [97] Once, no optimum conditions were observed in the response surface for both EE and PS only the identification of the region corresponding to the best response can be achieved.

The analysis of the figure 4.3 showed that there was a significant positive linear effect of P and T on the PS values meaning that when the encapsulation process was conducted at higher temperatures and higher pressure, the PS of the systems increased. [98–100] These results may be explained by the temperature dependent CO_2 solubility in beeswax mass. [87] [101] It is also observed that curcumin load and P have a positive effect on the EE, represented by an increase of EE with the increase of these two factors.

The best response can be achieved at 160 bar, 73 ºC and 10 % curcumin amount (wt%). Under these conditions the 65.4 µm resulting particles had a final curcumin load of 8.9 % with a span value of 1.7.

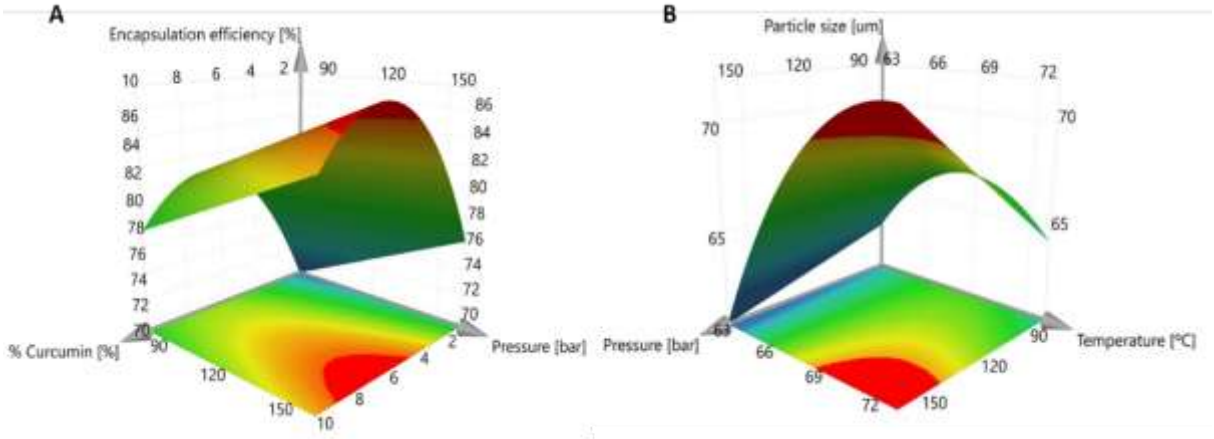

Figure 4.3| Fitted response surfaces to the A) EE, as a function of curcumin load and pressure and B) PS, as a function of temperature and pressure. Response surfaces plotted for two variables with the other fixed at middle settings.

Table 4.1| Summary of The CCFC design for the three independent variables and experimental results.

	independent variables			**Process responses**				
	Pressure (bar)	Temperature (ºC)	%Curcumin	Encapsulation efficiency (%)	Particle size (0,5)	Span	Average (% Load)	Error (%)
1	80	63	1	72,61 ± 1,74	65,604	1,866	0,73	2,40
2	160	63	1	62,33 ± 2,20	65,595	1,775	0,62	3,53
3	80	73	1	63,60 ± 0,98	66,386	1,773	0,64	1,53
4	160	73	1	82,43 ± 1,13	78,135	1,598	0,82	1,37
5	80	63	10	74,98 ± 1,78	59,154	1,794	7,50	2,37
6	160	63	10	87,93 ± 2,25	55,658	1,824	8,79	2,56
7	80	73	10	73,48 ± 3,68	60,827	1,782	7,35	5,01
8	160	73	10	89,75 ± 2,23	65,441	1,722	8,98	2,49
9	80	68	5,5	84,05 ± 2,88	67,052	1,773	4,62	3,42
10	160	68	5,5	85,76 ± 3,08	66,657	2,048	4,72	3,59
11	120	63	5,5	90,28 ± 1,78	62,439	2,009	4,97	1,97
12	120	73	5,5	77,51 ± 3,40	69,820	1,829	4,26	4,39
13	120	68	1	83,05 ± 1,05	82,293	1,755	0,83	1,26
14	120	68	10	82,51 ± 2,59	65,207	1,751	8,25	3,14
15	120	68	5,5	79,86 ± 2,47	58,150	1,999	4,39	3,10
16	120	68	5,5	85,07 ± 4,14	66,973	1,684	4,68	4,87
17	120	68	5,5	82,46 ± 1,57	70,185	1,757	4,54	1,91

Table 4.2| Model equations for the response profiles fitted to the values of EE and PS as a function P, T and %C, and respective R^2 and R_{adj}^2.

Polynomial model equation	R^2	R_{adj}^2
EE = 83,57 - 6,821 $[\%C]^2$	0,465	0,342
PS = 68,0739 + 3,2159 T - 5,1726 [%C]	0,699	0,518

4.1.2.Solid lipid nanoparticles and nanoemulsions

Both formulations at the nanoscale were produced and characterized by Universidade do Minho (Portugal) within the project PTDC/AGRTEC/5215/2014 financed by Fundação para a Ciência e Tecnologia.

To produce curcumin nanoemulsions prepared through high pressure homogenization, see 3.1.1.1, several biosurfactants were tested. Therefore, nanoemulsions produced with 0.1% of curcumin, LCT / MCT and 2.5% of Tween® 80 were selected for the next tasks. Beeswax (3%) SLP were prepared by ultra-homogenization with lecithin (1.5 %) and curcumin (0.1 %).

4.1.3.Physical chemical characterization

4.1.3.1. Size and morphology

As mentioned above, after the parameter optimization an amount of 5g of beeswax and curcumin (90:10 (w/w)) were precipitated through PGSS® (Figure 4.4) according to the best conditions obtained in the modelling. Microparticles characterisation are present in table 4.3.

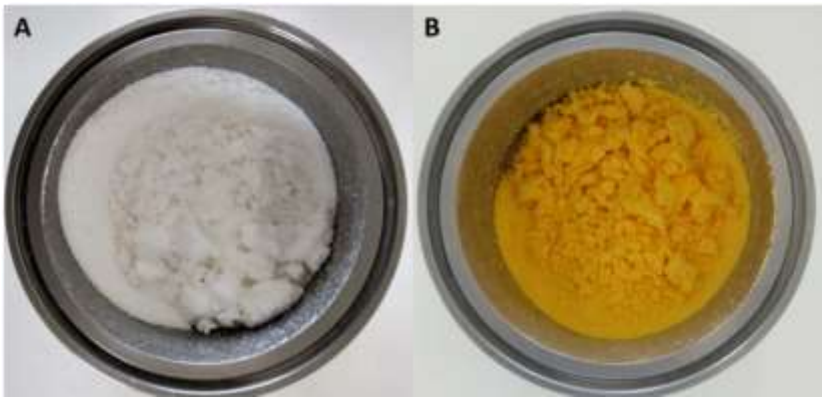

Figure 4.4| Final particles resulting from the use of optimized production parameters through RSM. A) Empty beeswax particles; B) Curcumin loaded microparticles produced with 10% curcumin (w/w).

Particle size is a critical factor for all drug delivery systems being one of the factors that control the kinetics of drug release. Ideally, to oral application, it is desired to obtained particles as smaller as possible to obtain a higher surface area used to enhance the dissolution rate.[27,102,103] Microparticulate curcumin system produced by PGSS® showed an average size of 65.44 µm measured by DLS with little

narrow size distribution pattern represented by the span value and confirmed in the SEM images (Figure 4.5). According to other studies of encapsulation using PGSS®, the mean particle sizes ranged between 4 and 100 µm. with the aim to reduce particle size were obtained positive results in relation to the literature. [45,104,105]

Table 4.3| Microparticles characterisation.

System: Beeswax/Curcumin	
EE	89,75 ± 2,23
Final Load (%)	8,98 ± 0,22
PS (µm)	65,44
Span	1,72

As pressure is increased, larger amounts of CO_2 are dissolved in the melted carrier. Therefore, due to higher-pressure drop across the nozzle, more CO_2 gas bubbles are formed increasing the cooling rate which originates porous particles as the gas cannot diffuse out of the particles perforating particle surface. [45,99] The micrographs show porous particles, of which are agglomerated forming aggregates. the non-exposure of curcumin crystals corroborates with the result obtained for the efficiency of encapsulation (89%) showing that it is encapsulated in its entirety.

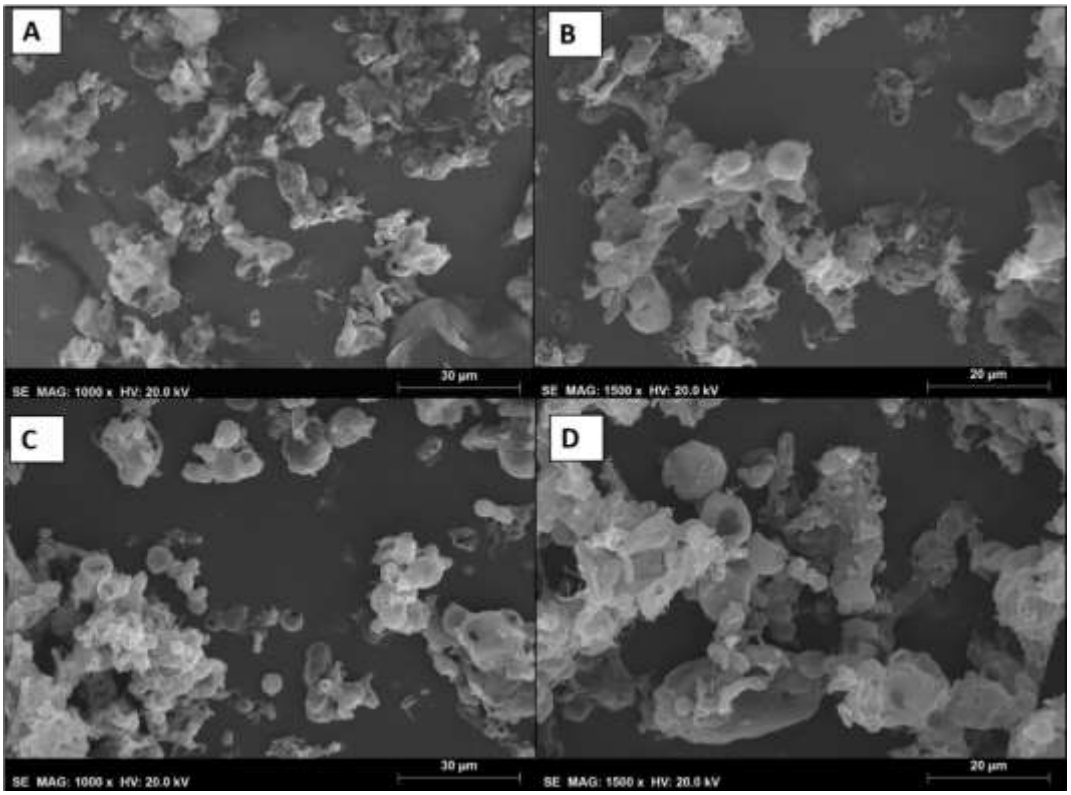

Figure 4.5| SEM micrographs of blank and loaded curcumin particles produced by PGSS® (nozzle diameter d=250µm); A) blank SLM at 1000x and B) 1500x magnification; C) curcumin loaded SLM at 1000x and D) 1500x magnification; Effect of operating conditions.

To emulsions-based curcumin particulate system, minimal average diameter obtained was approximately 150 nm obtained through SLN and MCT emulsions. The monodispersity of the nanoemulsions can be evaluated by its PDI, which can range from 0 to 1 (being 0 monodisperse and 1, polydisperse). The standard deviation of the average size measured was very small which presuppose a small variation in the particles size distribution. A large particle size distribution, also observed by the span value, is an important factor for the release kinetics of the compound. A higher dispersion value represents distinct values of release kinetics. This type of distribution is usual in SLN obtained by high shear homogenization method [106].

4.1.3.2. Zeta potential

The surface charge (zeta potential) of the droplet, as well as the interfacial free energy interaction, are the parameters which determine the electrostatic repulsive interactions between particles. The zeta potential values more electronegative than -30 mV and more positive than +30 mV generally represent sufficient electrostatic repulsion for stability. [107,108] By the analysis of table 4.4, it is possible to settle that the MCT based emulsion would be the only one formulation considered stable once features a -32.5 mV surface charge.

Table 4.4| Characterization of the emulsion-based curcumin nanoparticles.

Formulation	PS (nm)	Zeta potential (mV)	PDI
SLN	150,0	-20,5	0,27
LCT emulsion	184,1	-0,9	0,23
MCT emulsion	152,3	-32,5	0,20

4.1.3.3. Thermal behaviour – DSC measurements

After obtaining the solid lipid microparticles, DSC measurements were performed on curcumin structures and its isolated compounds. The melting point of the beeswax determined by melting point depression was confirmed by DSC analysis, on the other hand native curcumin endothermic peak was found approximately at 178 ºC, like reported in literature. [109,110]

Regarding the samples obtained by PGSS® processing, the most significant result is the maintenance of the characteristic melting peaks of the pure compounds in the mixture. That suggests a maintenance of physical properties which may be indicative of a phase separation. This confirms that the solid lipid matrix is heterogeneous, with an evident phase separation or crystallization of the two components, probably due to the saturation of the solid lipid matrix with curcumin. The presence of the bioactive compound in crystalline form within SLM hinders its solubilization. However, if the drug is in the amorphous state or in the disordered crystalline phase, easy diffusion of the drug molecules may occur through the polymer matrix, leading to sustained release of the encapsulated drug (Figure 4.6).

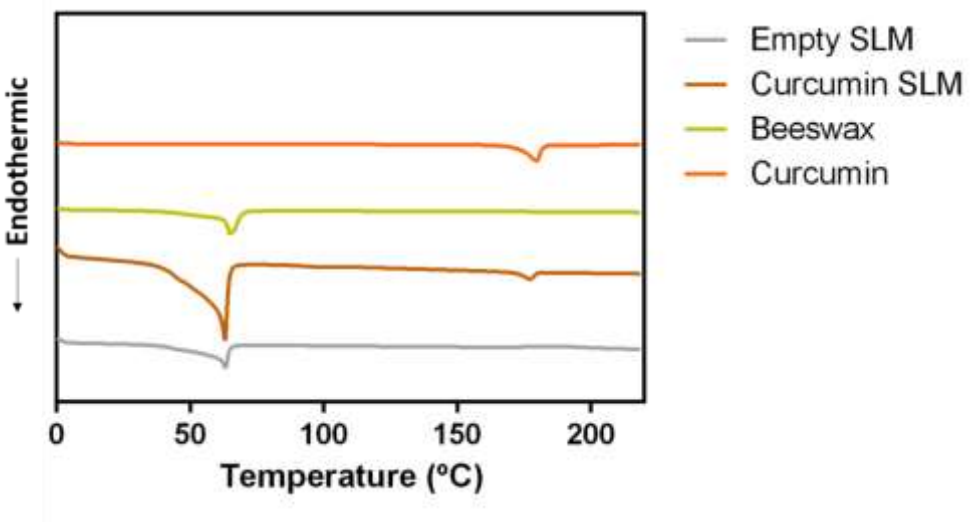

Figure 4.6| DSC thermographs of pure compounds and Solid lipid microparticles. Products of supercritical encapsulation of curcumin, loaded and not loaded with curcumin.

4.1.3.4. Dissolution study

At the end of 72 h close to 6 % (w/w) of the total concentration of encapsulated curcumin was released into the digestive fluids. However, this value is found to be 1.6x higher than the solubility of free curcumin in the same fluids. This results are supported by work of C. Jantarat et al. [111] The two-fluid test was performed to mimic the conditions of an IVD (2h of SGF action followed by 2h more with SIF). Once again the dissolution of curcumin of the particulate system was superior to free form, with this release being sharped at 72h.[112] All results are expressed in figure 4.7.

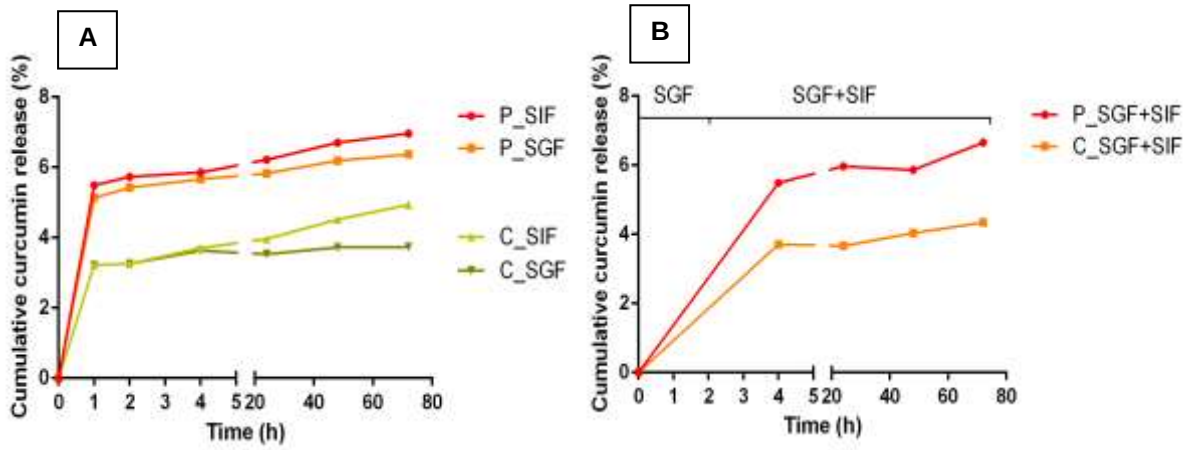

Figure 4.7| Dissolution profiles of curcumin (C) and curcumin encapsulated microparticles (P). A) in SIF, SGF and B) SGF plus SIF at 37 ± 0.2 °C during 72h at constant agitation (50 rpm).

4.1.3.5. In vitro digestion: impact on SLM and emulsions

To better mimic the intestinal process, microparticles loaded with curcumin underwent an in vitro digestion described in 3.4. In this process an initial amount of 400 mg of microparticles with 35.92 mg

of encapsulated curcumin were used. After digestion the final concentration of 3.5 ± 0.35 µg/mL of curcumin was quantified in solution, corresponding a total of 140 µg in final digested solution.

After the digestion assay the quantified curcumin concentration was much lower than the initial amount. In gastric digestion process the synergistic interactions between enzymes and acidic alkaline conditions result in a significant breakdown of solid lipid microparticles. These oscillation of pH values from the gastric phase to the end of the intestinal phase can cause hydrolysis of free and encapsulated curcumin resulting in compound degradation. Literature show that curcumin is unstable in phosphate buffer at pH 7.4 and stabilizes strongly with the decrease of pH. [106,108,113]

Curcumin, which is soluble only in the organic solvents, remained encapsulated in the separated hydrophobic particles, and with this reduced surface area, the digestive enzymes will not have acted to enable mixed micelle formation, thus reducing bioavailability. In general, the formulation was able to promote a strong enzymatic protection to the bioactive compound evidenced by the low amount of released in solution. However, the quantification is preceded by a filtration step which may have promoted the retention of part of the compound to be detected in the filter together with the debris and digestion compounds.

Emulsion based nanoparticles after subjected to IVD were characterized through the effective bioavailability, stability and nanostructure behavior (size, ζ-potential and FFA). All nanostructures presented to be stable until gastric phase, where it was observed an increase of the nanostructures size. Although all nanostructures, excepting SLN, presented a decrease of size in the intestinal phase, the polydispersity index was too high (i.e., >0.4).

Table 4.5| Characterization of solid lipid nanoparticles before and after IVD.

		PS (nm)	PDI	Curcumin (µg/mL)
SLN curcumin loaded	Non-Digested	137.7	0.264	99.90
	Digested	392.4	0.589	6.71
Blank SLN	Non-Digested	141.7	0.254	
	Digested	528.1	0.554	

All three formulations presented a negative or close to zero ζ-potential value before digestion process and after oral phase. However, at gastric phase, they showed a positive or close to zero ζ-potential value, probably due to pH and ionic strength changes. At intestinal phase, they presented a negative ζ-potential value due to pH increase. (Data not show)

Considering FFA determination, the nanoemulsions presented a higher curcumin concentration than the SLN, showing that the oil physical state can influence the curcumin bioaccessibility. Once the nanoemulsions are composed by the liquid lipid, the lipase can break the lipid chains more easily than the solid lipid used in the SLN. Comparing the different triglyceride's chains size, it was possible to observe that the nanoemulsions produced with MCT, NE-MCT, showed a higher FFA concentration than nanoemulsions produced with LCT, NE-LCT, showing that triglyceride's chain size can also influence the curcumin bioaccessibility. NE-LCT showed a higher curcumin bioaccessibility when compared to SLN and NE-MCT. However, NE-LCT presented a lower curcumin's stability than NE-MCT, showing that the NE-MCT better protected the curcumin against degradation and consequently, it showed a higher effective bioavailability

4.1.3.6. Cytotoxicity assay

Before carrying out the curcumin permeation study the best formulation were subjected to several tests of cellular cytotoxicity by the MTS method described in 3.5.2.1. To evaluate the toxicity of the compounds, curcumin and curcumin loaded-particles were tested as "solution" and "dispersion", respectively. The curcumin solution to be tested was prepared by pre-dissolving the pure compound in ethanol p.a and then applied to the cell monolayer. The particles, in turn, were tested by "dispersion". That consisted of pouring the compound directly into the cell culture medium. All assays disclosed were performed on Caco-2 confluent cells.

First, the cytotoxicity study of free curcumin was carried out to compare the results with curcumin particulate systems and to observe the impact of the different formulations on their cytotoxicity.

The results of the cytotoxicity experiments revealed that the dispersion test for curcumin microparticles did not show toxicity in the range of concentrations tested relatively to control (100% cell viability, culture medium) after 24h incubation. However, the samples of curcumin floated and formed aggregates into the wells which prevented a direct contact with the cellular monolayer. Still

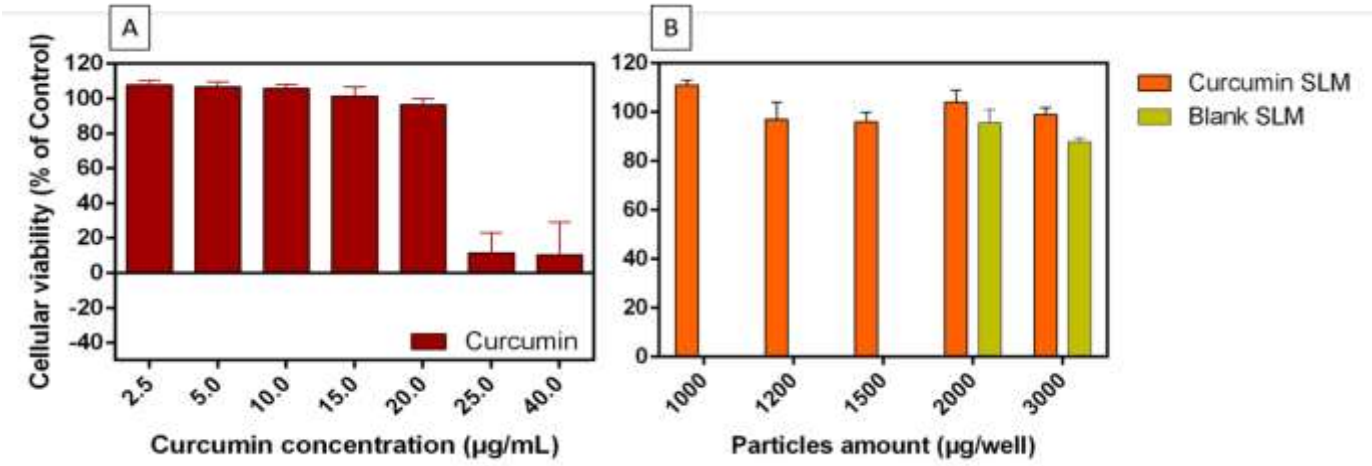

Figure 4.8| Cytotoxicity assay using MTS reagent. Incubation of curcumin formulations in Caco-2 cell line during 24h at 37 ºC and 5% CO2 humidified atmosphere. Solution of 100 % (v/v) of culture medium in cell culture was used as a positive, none cytotoxic, control. A) Free curcumin; B) Curcumin solid lipid microparticles blank and loaded produced by PGSS® technique.

microparticles unload caused slight cell death and decreased cell viability, at the maximal concentrations tested, for 90%. On the other hand, the pure compound in a concentration of 25 µg/mL decreased cell viability by 88.5% and was therefore considered toxic to cells (Figure 4.8). Although MTS results are influenced not only by the incubation time but also by the cell type, the cell number and the ratio of MTS detection reagents to cells in culture [114], these native curcumin toxicity values are in agreement with the values found in the literature for different cell lines. [115]

To determine changes in curcumin microparticle cytotoxicity after IVD and to estimate a non-toxic concentration for following permeation studies, differentiated Caco-2 cells were exposed for 24 h to the digested particles. The results for cell viability after 24 h exposure are presented in Figure 4.9. This procedure was performed as a function of the amount of curcumin in solution after IVD and resulted in a strong cell death at concentrations above 1 µg/ml. So, a non-toxic concentration of 0.5 and 1 µg/ml was chosen for the subsequent studies.

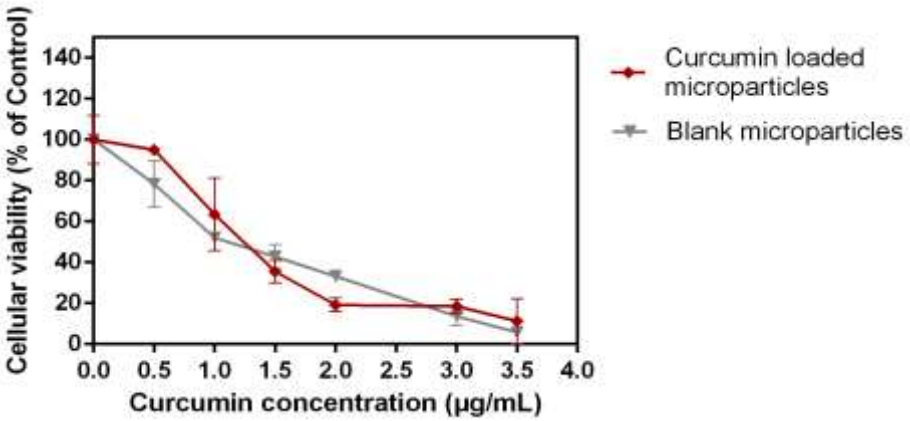

Figure 4.9| Cytotoxicity assay using MTS reagent. incubation of all digested microparticles, loaded and empty, in Caco-2 cell line during 24h at 37 ºC and 5% CO2 humidified atmosphere. Solution of 100 % (v/v) of culture medium in cell culture was used as a positive, none cytotoxic, control.

A first nanoemulsion formulation, composed of lecithin (2.25%), MCT oil (10%), curcumin (0.01%) and water was tested before and after undergoing the in vitro digestion process. Cytotoxicity assays have shown that before the in vitro digestion the nanoemulsion loaded and unloaded does not

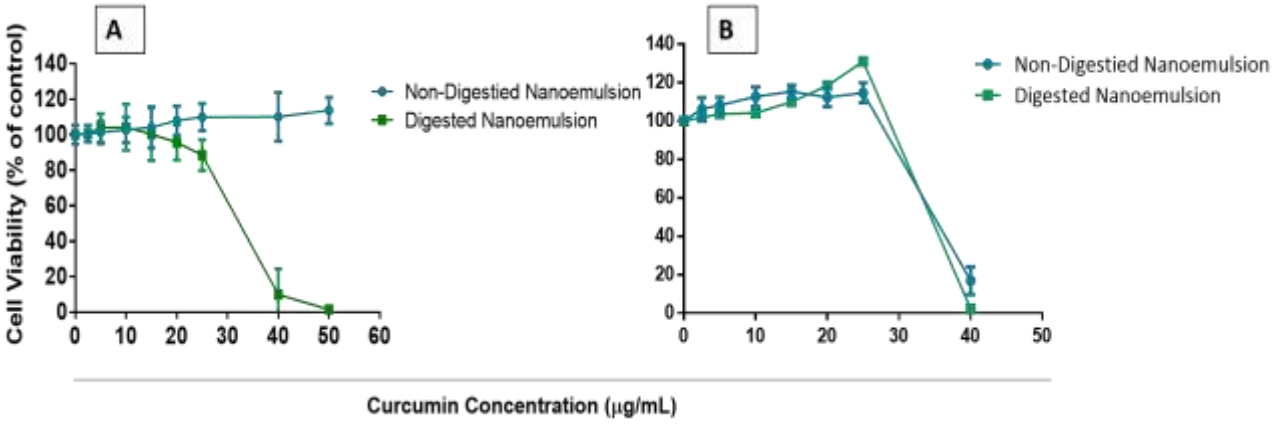

Figure 4.10| Cytotoxicity assay using MTS reagent: incubation in Caco-2 cell line during 24h at 37 ºC and 5% CO_2 humidified atmosphere. Solution of 100 % (v/v) of culture medium in cell culture was used as a positive, none cytotoxic, control. A) MCT based emulsions; B)LCT based emulsions.

present cell cytotoxicity (Figure 4.10). In contrast, the nanoemulsion after in vitro digestion process showed high cytotoxicity from 40 µg/mL of curcumin equivalents leading to the destruction of the cellular monolayer. Since this cytotoxicity was only observed in the digested ones, the isolated excipients used in the formulations were tested also before and after in vitro digestion to determine which would be contributing to the cytotoxic effect. The results showed that the digested MCT oil, in percentages used in the formulation, was cytotoxic to Caco-2 cells, while lecithin retains its non-cytotoxic profile in both

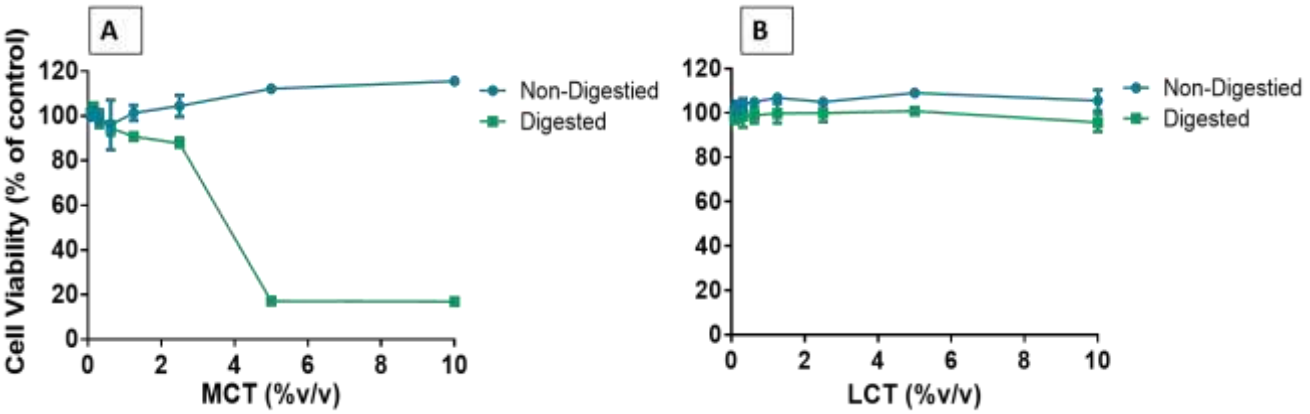

Figure 4.11| Cytotoxicity assay using MTS reagent: incubation in Caco-2 cell line during 24h at 37 ºC and 5% CO2 humidified atmosphere. Solution of 100 % (v/v) of culture medium in cell culture was used as a positive, none cytotoxic, control. A) MCT and B) LCT oil excipient.

conditions (Figure 4.11). Thus, in the search for an alternative to this excipient LCT oil was selected and tested, resulting in a non-cytotoxic profile to the cells (Figure 4.11). However, this new formulation, prepared with the LCT excipient, showed a decrease in cell viability at the highest tested concentrations (Figure 4.10). These results may, not indicate direct cytotoxicity of the formulation and be the result of the deposition of the nanostructures on the cell monolayer, preventing the correct gas exchanges, since the nanoemulsion showed a high opacity at higher concentrations.

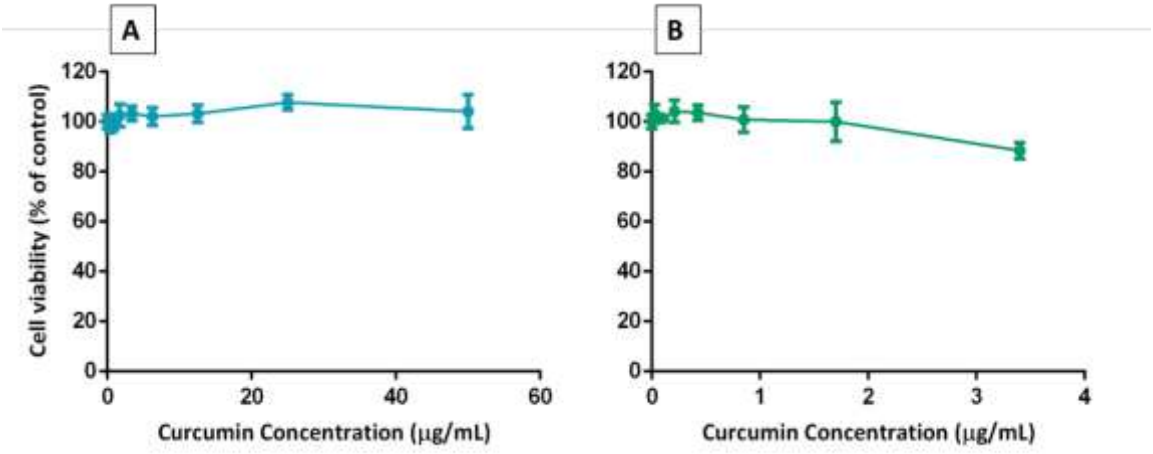

Figure 4.12| Cytotoxicity assay using MTS reagent: incubation of all nanoemulsions compounds in Caco-2 cell line during 24h at 37 ºC and 5% CO2 humidified atmosphere. Solution of 100 % (v/v) of culture medium in cell culture was used as a positive, non-cytotoxic, control. A) SLM non-digested and B) digested ones.

The results referent to non-digested particles are in full agreement with the literature where the cytotoxicity of SLN prepared with triglycerides and containing lecithin was tested on various cell lines and does not express any of cellular toxicity. [115–118].

Next, cytotoxicity tests were started with SLN (beeswax (3%), lecithin (1.5%), Tween 80 (1.5%), curcumin (0.1%)) and the results showed that both SLN before and after in vitro digestion were not cytotoxic for Caco-2 cells at all concentrations tested with only a slight decrease of the cellular viability to 90% at the higher concentration of the digest one, 3.5 μg/mL of curcumin (Figure 4.12).

4.2. Validation and characterization of the *in vitro* model of human intestinal epithelium

4.2.1.Mucus identification

In this study with the aim of elaborating a co-culture to mimic the intestinal epithelium the production of mucus by the HT29-MTX-E12 cell line cultured together with the Caco-2 enterocytes was stablished. The cells were characterized regarding the formation of a confluent monolayer, since it is known that mucus strongly impacts the mobility of nanoparticles. To detect the production of mucus alcian blue staining of the mucins produced by the cells was carried out (Figure 4.13). [55] Transwell® plates were inoculated and TEER was measured every time before the staining to prevent cell viability.

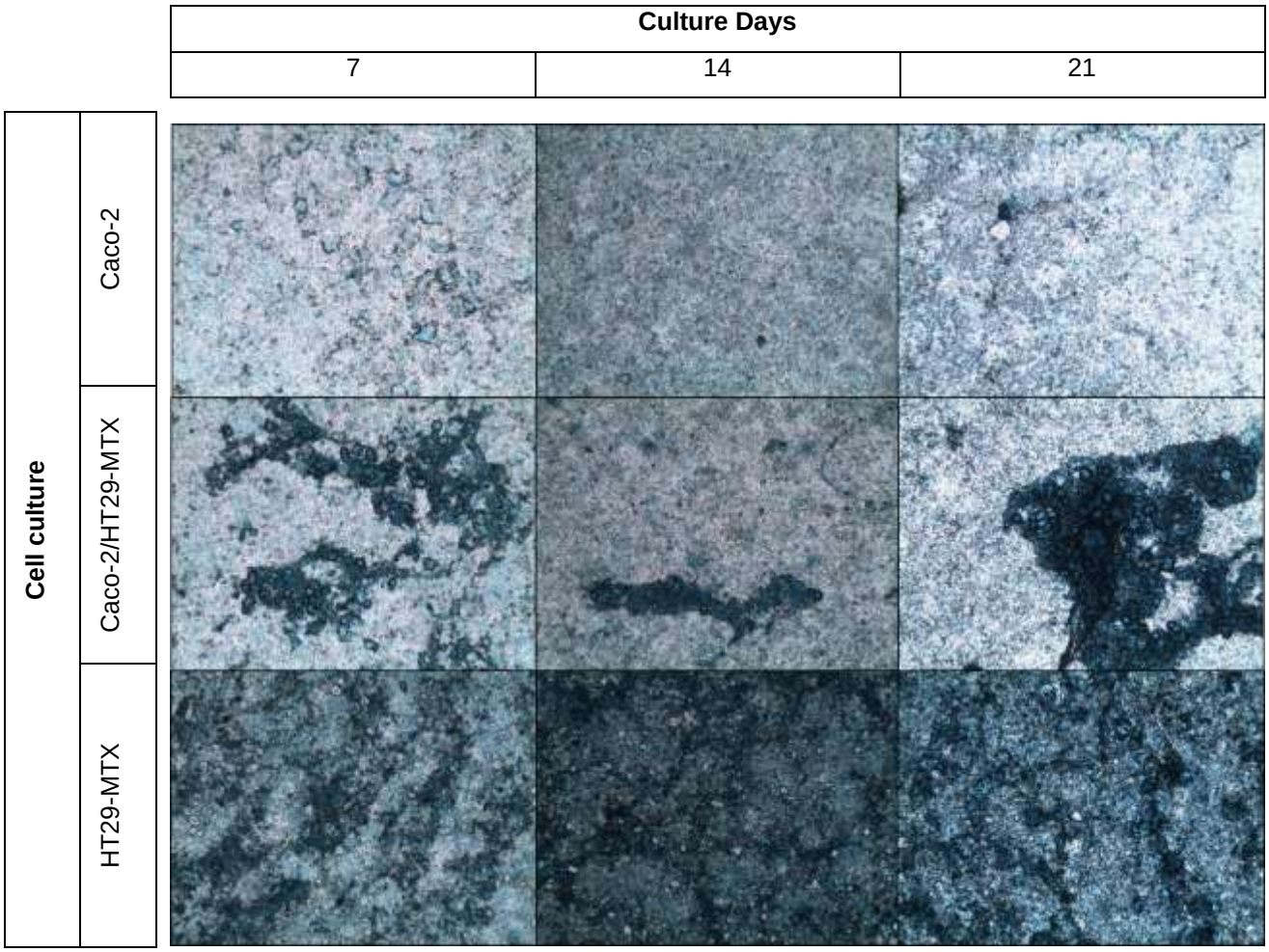

Figure 4.13| Staining of mucus present in Caco-2 and HT29-MTX monolayer and co-culture. Staining at 7, 14 and 21 days on a Transwell® plate.

The proportion between Caco-2 and HT29-MTX cells, like the *in vivo* situation, is one of the most important details for co-culture implementation. According to the work of *Araújo et al.* [55], the ratio used was 9:1 respectively. Caco-2 cells co-cultured displayed slight variability in microvilli density which did not allow the undoubted confirmation of the presence of HT29-MTX cells. Nonetheless, HT29-MTX

cells contain intracellular mucin granules that allowed its identification due to residual evidences of mucus retained over the surface of microvilli by SEM.

Alcian blue is a basic dye that allows the detection of cellular acidic mucin glycoproteins. When it binds whit, affinity provides a strong blue color.[119] To perform mucus staining duly differentiated cells were used once it is necessary the production of cellular markers characteristic for the characterization of the model.

The mucus secretion by the HT29-MTX cells, both in mono or in the co-culture was confirmed and compared to Caco-2 monolayer since due to the lack of goblet cells these do not express the mucus layer. (Figure 4.14) Therefore, it was observed experimentally that HT29-MTX cells can maintain their intrinsic properties, producing mucus not only when in monocultures but also when grown together with Caco-2.

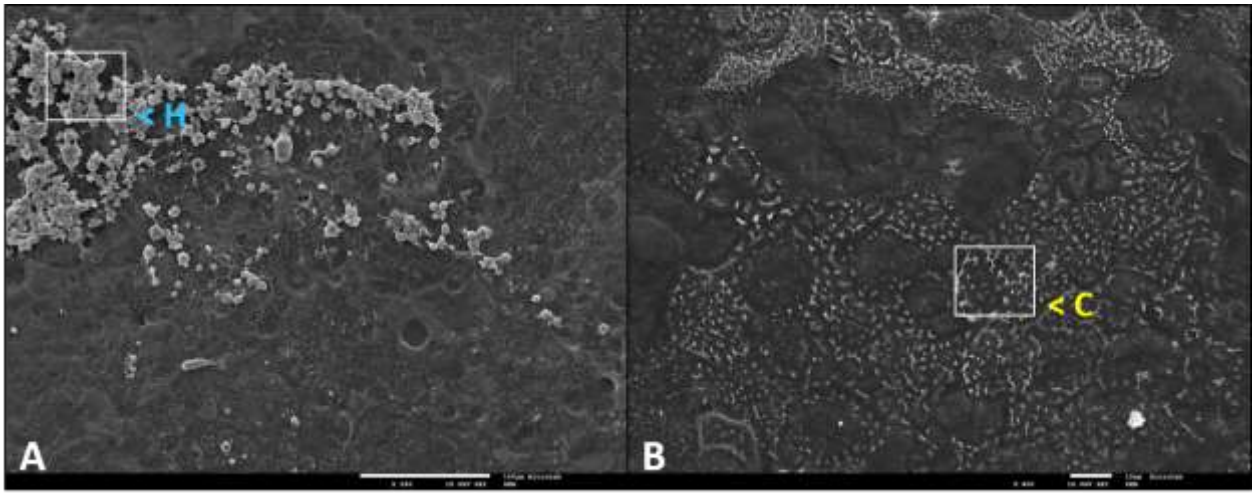

Figure 4.14|SEM analysis of the triple culture. (H) Mucus-secreting HT29-MTX cells were observed in the triple culture and were properly identified through the layer of mucus they produced. Compared with the caco-2 cells (C) with its characteristics tight junctions and microvilli.

4.2.2.Morphological features of M-like cells

To complete the characterization of the *in vitro* human intestinal epithelium it was essential to detect evidence of the presence of the M cell phenotype within the cell monolayers. In the absence of any specific human M-cell marker discrimination of M cells within cell monolayers was based on morphological criteria. The microvilli-free morphology of M cells was used to identify them by SEM (Figure 4.15). [120] [54]

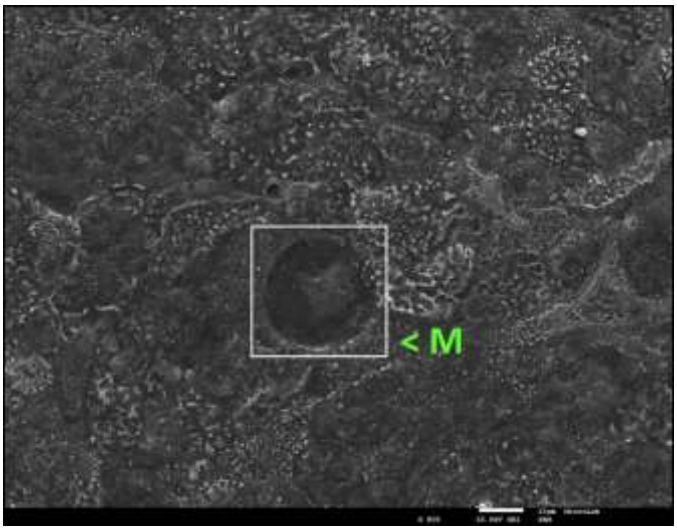

Figure 4.15| SEM analysis of the triple culture. M cells (M) were identified due to their lack of microvilli in contrast to Caco-2 cells.

4.3. Curcumin permeability studies

Initial studies on the passive absorption of a series of compounds across Caco-2 cells indicated that Caco-2 monolayers may be a useful model for drug absorption studies. After the entire process of implementation and characterization of the co-culture, as well as all the cytotoxicity assays of all the compounds used, permeability tests were performed. These were designed to compare the transport through the monolayer of free curcumin and encapsulated in micro solid lipid microparticles, digested and undigested. The assay was performed simultaneously on a differentiated Caco-2 and a triple co-culture monolayer.

The low particle size confirmed that, all tree formulations, are suitable for enabling gastrointestinal absorption by M-cells on Peyer's patches. The transport by M-cells is size dependent and are able to transport nanoparticles with sizes in the range of 200 nm. [113] The measurement of TEER values was employed as an integrity evaluator of the monolayer formed and it was monitored during the assay. The intrinsic resistance of the cell layer is influenced by the cell culture medium in the apical and basolateral compartment, by the membrane of the filter inserts and by the electrode interface. Since transport experiments are performed in HBSS, TEER values typically decreased in result of the adjustment of the experiment conditions even so the values, before the experiment, for all wells were above 700 Ω cm^2 (n=4) (Figure 7.3).

During the assay a difference in TEER values between the monolayer of caco-2 and the triple co-culture was observed. Since the decrease of this value presupposes the existence of cellular transport, this fact may be related to the increase in the transepithelial transport promoted by the M cells in the co-culture as well as the diminution of tight junctions due to the conversion of Caco-2 cell into M cells. [54,121,122]

The maximum nontoxic amount of free curcumin, 20 µg/mL, was added to the apical site of the Transwell® plate and a 0.1008 x 10^{-6} cm/s value of P_{app} (eq.2) was calculated from apical to basolateral site. [123–125] As for the analysis of encapsulated curcumin permeability, the results obtained by HPLC were below detection limits. However, a small peak appears at the same retention time of the curcumin. [18] Drugs that are completely absorbed in humans have permeability coefficients >1x10^{-6} cm/s. while compounds that are less absorved, > 1% but < 100%, have permeability coefficients of 0.1 - 1.0x10^{-6} cm/s. One the other hand the ones that are absorbed to < 1% had permeability coefficients of 11 x 10-7 cm/s. [57]

Many incompletely absorbed compounds are not absorbed across the cell membranes, i.e. they are excluded from the transcellular pathway, Instead, they are absorbed by the alternative paracellular pathway (across the tight junctions between the cells). The paracellular pathways in colonic epithelium are tighter than in small intestinal epithelium. The area of the peaks was determined, and it was evident that in the co-culture due to the presence of M cells the curcumin transport through the membrane was 5.6x larger than in Caco-2 model (Figure 7.2). This result is due to the role of the mucus layer, expressed in the co-culture, with the uptake of the particulate systems. Confirming the support and protection for the intestinal epithelium. This uptake may also be responsible for the release of the compounds over time and increase their cellular bioavailability.

5. Conclusions

In this study, several formulations were tested with the aim of increasing the cellular availability and stability of curcumin. Microformulations were produced using supercritical CO_2 technique, particles from gas saturated solutions, and nanoformulations were based on triglyceride emulsions (LCT and MCT). These formulations underwent a digestive enzymatic process to mimic the digestion process that occurs in the intestinal epithelium. Subsequent cellular tests were performed on a validated triple co-culture based on Caco-2, HT29-MTX-E12, and Raji B lymphocytes, to closely mimic the monolayer of the human intestinal epithelium.

Beeswax solid lipid microparticles entrapping curcumin were successfully produced by PGSS process with an encapsulation efficiency of 89.75 ± 2.23 % and a curcumin load of 8.98 % (w/w). Curcumin loading values were obtain as high as those obtained by traditional SLN®/SLM emulsions-based methods, but with all advantages of supercritical fluid technology. This process assigned curcumin protection, represented in IVD, as well as increased cell availability. Although the formulation presented some curcumin concentration dependent toxicity in Caco-2 monolayer assay.

A triple co-culture model validation took place, using the human colon adenocarcinoma Caco-2 cells cultivated with HT29-MTX-E12 epithelial cells in a 9:1 ratio to produce the intestinal epithelium mucus layer to which Raji B lymphocytes added M-cells like phenotype.

Results demonstrate that Caco-2/HT29/Raji B triple co-culture may be used in the future to obtain a simulated intestinal barrier, with mucus-producing properties and M cells of Peyer's patches to study bioactives absorption, both in solution or associated with carriers. Furthermore, we confirmed that nanoparticle uptake is strongly impacted by the mucus interaction with particulate systems, with the higher uptake amounts attributed to the presence of M cells compared to single Caco-2 monolayers. This result confirms the importance of an *in vitro* culture that express the epithelial mucus layer for compounds oral administration study of bioavailability and stability.

6. References

1. Espín, J. C., García-Conesa, M. T. & Tomás-Barberán, F. A. Nutraceuticals: Facts and fiction. *Phytochemistry* **68,** 2986–3008 (2007).
2. Zhao, J. Nutraceuticals, Nutritional Therapy, Phytonutrients, and Phytotherapy for Improvement of Human Health: A Perspective on Plant Biotechnology Application. *Recent Pat. Biotechnol.* **1,** 75–97 (2007).
3. Bernal, J., Mendiola, J. A., Ibáñez, E. & Cifuentes, A. Advanced analysis of nutraceuticals. *J. Pharm. Biomed. Anal.* **55,** 758–774 (2011).
4. Shahidi, F. Functional Foods : Their Role in Health Promotion and Disease Prevention. *J. Food Sci.* **69,** 146–149 (2004).
5. Zeisel, S. H. Regulation of "nutraceuticals". *Science* **285,** 1853–5 (1999).
6. Coppens, P., Da Silva, M. F. & Pettman, S. European regulations on nutraceuticals, dietary supplements and functional foods: A framework based on safety. *Toxicology* **221,** 59–74 (2006).
7. Brower, V. Nutraceuticals: Poised for a healthy slice of the healthcare market? *Nat. Biotechnol.* **16,** 728–731 (1998).
8. Joe, B., Vijaykumar, M. & Lokesh, B. R. Biological Properties of Curcumin-Cellular and Molecular Mechanisms of Action. *Crit. Rev. Food Sci. Nutr.* **44,** 97–111 (2004).
9. Priyadarsini, K. I. Photophysics, photochemistry and photobiology of curcumin: Studies from organic solutions, bio-mimetics and living cells. *J. Photochem. Photobiol. C Photochem. Rev.* **10,** 81–95 (2009).
10. Ishita, C. & Khaushik, B. Turmeric and Curcumin: Biological Actions and Medical Applications (Review). *Curr. Sci.* **87,** 44–50 (2004).
11. Strimpakos, A. S. & Sharma, R. A. Curcumin: Preventive and Therapeutic Properties in Laboratory Studies and Clinical Trials. *Antioxid. Redox Signal.* **10,** 511–546 (2008).
12. Kawamori, T. *et al.* Chemopreventive Effect of Curcumin , a Naturally Occurring Anti-Inflammatory Agent , during the Promotion / Progression Stages of Colon Cancer Chemopreventive Effect of Curcumin , a Naturally Occurring Anti-Inflammatory Agent , during the Promotion / Prog. 597–601 (1999).
13. Anand, P. *et al.* Bioavailability of Curcumin : Problems and Promises reviews Bioavailability of Curcumin : Problems and Promises. *Mol. Pharmacol.* **4,** 807–818 (2007).
14. Aggarwal, B. B. & Harikumar, K. B. Potential therapeutic effects of curcumin, the anti-inflammatory agent, against neurodegenerative, cardiovascular, pulmonary, metabolic, autoimmune and neoplastic diseases. *Int. J. Biochem. Cell Biol.* **41,** 40–59 (2009).
15. Zebib, B., Mouloungui, Z. & Noirot, V. Stabilization of curcumin by complexation with divalent cations in glycerol/water system. *Bioinorg. Chem. Appl.* **2010,** (2010).
16. Food, E. & Authority, S. Refined exposure assessment for curcumin (E 100). *EFSA J.* **12,** n/a-n/a (2014).
17. Downham, A. & Collins, P. Colouring our foods in the last and next millennium. *Int. J. Food Sci. Technol.* **35,** 5–22 (2000).
18. Jayaprakasha, G. K., Rao, L. J. M. & Sakariah, K. K. Improved HPLC method for the determination of curcumin, demethoxycurcumin, and bisdemethoxycurcumin. *J. Agric. Food Chem.* **50,** 3668–3672 (2002).
19. Li, S. *et al.* Chemical Composition and Product Quality Control of Turmeric (Curcuma longa L .). 28–54 (2011).
20. Wichitnithad, W., Jongaroonngamsang, N., Pummangura, S. & Rojsitthisak, P. A simple isocratic HPLC method for the simultaneous determination of curcuminoids in commercial turmeric extracts. *Phytochem. Anal.* **20,** 314–319 (2009).
21. Wang, Y. J. *et al.* Stability of curcumin in buffer solutions and characterization of its degradation products. *J. Pharm. Biomed. Anal.* **15,** 1867–1876 (1997).

22. Ray, S., Raychaudhuri, U. & Chakraborty, R. An overview of encapsulation of active compounds used in food products by drying technology. *Food Biosci.* **13,** 76–83 (2016).

23. Gibbs, B. F., Kermasha, S., Alli, I. & Mulligan, C. N. Encapsulation in the food industry: A review. *Int. J. Food Sci. Nutr.* **50,** 213–224 (1999).

24. Nedovic, V., Kalusevic, A., Manojlovic, V., Levic, S. & Bugarski, B. An overview of encapsulation technologies for food applications. *Procedia Food Sci.* **1,** 1806–1815 (2011).

25. Jaspart, S., Piel, G., Delattre, L. & Evrard, B. Solid lipid microparticles: formulation, preparation, characterisation, drug release and applications. *Expert Opin. Drug Deliv.* **2,** 75–87 (2005).

26. Odriozola-Serrano, I., Oms-Oliu, G. & MartÃ-n-Belloso, O. Nanoemulsion-Based Delivery Systems to Improve Functionality of Lipophilic Components. *Front. Nutr.* **1,** 1–4 (2014).

27. Ahmed, K., Li, Y., McClements, D. J. & Xiao, H. Nanoemulsion- and emulsion-based delivery systems for curcumin: Encapsulation and release properties. *Food Chem.* **132,** 799–807 (2012).

28. Silva, H. D., Cerqueira, M. Â. & Vicente, A. A. Nanoemulsions for Food Applications: Development and Characterization. *Food Bioprocess Technol.* **5,** 854–867 (2012).

29. Anton, N. & Vandamme, T. F. The universality of low-energy nano-emulsification. *Int. J. Pharm.* **377,** 142–147 (2009).

30. Pinheiro, A. C. *et al.* Unravelling the behaviour of curcumin nanoemulsions during in vitro digestion: effect of the surface charge. *Soft Matter* **9,** 3147 (2013).

31. Weiss, J. *et al.* Solid lipid nanoparticles as delivery systems for bioactive food components. *Food Biophys.* **3,** 146–154 (2008).

32. Mehnert, W. & Mäder, K. Solid lipid nanoparticles: Production, characterization and applications. *Adv. Drug Deliv. Rev.* **64,** 83–101 (2012).

33. Wissing, S. A., Kayser, O. & Müller, R. H. Solid lipid nanoparticles for parenteral drug delivery. *Adv. Drug Deliv. Rev.* **56,** 1257–1272 (2004).

34. Pasquali, I. & Bettini, R. Are pharmaceutics really going supercritical? *Int. J. Pharm.* **364,** 176–187 (2008).

35. Moquin, P. H. L. & Sun, M. *Supercritical Fluid Extraction of Nutraceuticals and Bioactive Compounds*. (2008).

36. Tabernero, A., Martín del Valle, E. M. & Galán, M. A. Supercritical fluids for pharmaceutical particle engineering: Methods, basic fundamentals and modelling. *Chem. Eng. Process. Process Intensif.* **60,** 9–25 (2012).

37. Brunner, G. Supercritical fluids: Technology and application to food processing. *J. Food Eng.* **67,** 21–33 (2005).

38. Beckman, E. J. Supercritical and near-critical CO2in green chemical synthesis and processing. *J. Supercrit. Fluids* **28,** 121–191 (2004).

39. Martín, A. & Cocero, M. J. Micronization processes with supercritical fluids: Fundamentals and mechanisms. *Adv. Drug Deliv. Rev.* **60,** 339–350 (2008).

40. Nunes, A. V. M. & Duarte, C. M. M. Dense CO2 as a Solute, Co-Solute or Co-Solvent in Particle Formation Processes: A review. *Materials (Basel).* **4,** 2017–2041 (2011).

41. Jung, J. & Perrut, M. Particle design using supercritical fluids: Literature and patent survey. *J. Supercrit. Fluids* **20,** 179–219 (2001).

42. Jung, J. & Perrut, M. Particle design using supercritical fluids Literature and patent survey.pdf. *J. Supercrit. Fluids* **20,** 179–219 (2001).

43. Knez, Z. High pressure process technology-quo vadis? *Chem. Eng. Res. Des.* **82,** 1541–1548 (2004).

44. Knez, Z. & Weidner, E. Particles formation and particle design using supercritical fluids. *Curr. Opin. Solid State Mater. Sci.* **7,** 353–361 (2003).

45. Varona, S., Martín, Á., Cocero, M. J. & Duarte, C. M. M. Encapsulation of Lavandin Essential Oil

in Poly-(ε{lunate}-caprolactones) by PGSS Process. *Chem. Eng. Technol.* **36,** 1187–1192 (2013).

46. Martín, V. *et al.* Production of copper loaded lipid microparticles by PGSS®(particles from gas satured solutions) process. *J. Supercrit. Fluids* **131,** 124–129 (2018).

47. Fraile, M. *et al.* Production of new hybrid systems for drug delivery by PGSS (Particles from Gas Saturated Solutions) process. *J. Supercrit. Fluids* **81,** 226–235 (2013).

48. Weidner, E. High pressure micronization for food applications. *J. Supercrit. Fluids* **47,** 556–565 (2009).

49. Martín, Á., Pham, H. M., Kilzer, A., Kareth, S. & Weidner, E. Micronization of polyethylene glycol by PGSS (Particles from Gas Saturated Solutions)-drying of aqueous solutions. *Chem. Eng. Process. Process Intensif.* **49,** 1259–1266 (2010).

50. Morishita, M. & Peppas, N. A. Is the oral route possible for peptide and protein drug delivery? *Drug Discov. Today* **11,** 905–910 (2006).

51. Gomez-Orellana, I. Strategies to improve oral drug bioavailability. *Expert Opin. Drug Deliv.* **2,** 419–433 (2005).

52. Kompella, U. B. & Lee, V. H. L. Delivery systems for penetration enhancement of peptide and protein drugs: Design considerations. *Adv. Drug Deliv. Rev.* **46,** 211–245 (2001).

53. Porter, C. J. H., Trevaskis, N. L. & Charman, W. N. Lipids and lipid-based formulations: Optimizing the oral delivery of lipophilic drugs. *Nat. Rev. Drug Discov.* **6,** 231–248 (2007).

54. des Rieux, A. *et al.* An improved in vitro model of human intestinal follicle-associated epithelium to study nanoparticle transport by M cells. *Eur. J. Pharm. Sci.* **30,** 380–391 (2007).

55. Araújo, F. & Sarmento, B. Towards the characterization of an in vitro triple co-culture intestine cell model for permeability studies. *Int. J. Pharm.* **458,** 128–134 (2013).

56. Norris, D. A., Puri, N. & Sinko, P. J. The effect of physical barriers and properties on the oral absorption of particulates. *Adv. Drug Deliv. Rev.* **34,** 135–154 (1998).

57. Artursson, P. & Karlsson, J. Correlation between oral drug absorption in humans and apparent drug permeability coefficients in human intestinal epithelial (Caco-2) cells. *Biochem. Biophys. Res. Commun.* **175,** 880–885 (1991).

58. Travis, S. & Menzies, I. Intestinal permeability: functional assessment and significance. *Clin. Sci.* **82,** 471–488 (1992).

59. Johnson, L. R. *Regulation of gastrointestinal mucosal growth*. *World Journal of Surgery* **3,** (1979).

60. Araújo, F. *et al.* In vitro M-like cells genesis through a tissue-engineered triple-culture intestinal model. *J. Biomed. Mater. Res. - Part B Appl. Biomater.* **104,** 782–788 (2016).

61. Antunes, F., Andrade, F., Araújo, F., Ferreira, D. & Sarmento, B. Establishment of a triple co-culture in vitro cell models to study intestinal absorption of peptide drugs. *Eur. J. Pharm. Biopharm.* **83,** 427–435 (2013).

62. Lozoya-Agullo, I. *et al.* Usefulness of Caco-2/HT29-MTX and Caco-2/HT29-MTX/Raji B coculture models to predict intestinal and colonic permeability compared to Caco-2 monoculture. *Mol. Pharm.* **14,** 1264–1270 (2017).

63. Egan, W. J. & Lauri, G. Prediction of intestinal permeability. *Adv. Drug Deliv. Rev.* **54,** 273–289 (2002).

64. Sun, H., Chow, E. C., Liu, S., Du, Y. & Pang, K. S. The Caco-2 cell monolayer: usefulness and limitations. *Expert Opin. Drug Metab. Toxicol.* **4,** 395–411 (2008).

65. Lechanteur, A., Almeida, A. & Sarmento, B. Elucidation of the impact of cell culture conditions of Caco-2 cell monolayer on barrier integrity and intestinal permeability. *Eur. J. Pharm. Biopharm.* **119,** 137–141 (2017).

66. Shah, P., Jogani, V., Bagchi, T. & Misra, A. Role of Caco-2 cell monolayers in prediction of intestinal drug absorption. *Biotechnol. Prog.* **22,** 186–198 (2006).

67. Press, B. & Di Grandi, D. Permeability for intestinal absorption: Caco-2 assay and related issues. *Curr. Drug Metab.* **9,** 893–900 (2008).

68. Peterson, M. D. & Mooseker, M. S. Characterization of the enterocyte-like brush border cytoskeleton of the C2BBe clones of the human intestinal cell line, Caco-2. *J. Cell Sci.* **102 (Pt 3,** 581–600 (1992).

69. Hilgendorf, C. *et al.* Caco-2 versus Caco-2/HT29-MTX co-cultured cell lines: Permeabilities via diffusion, inside- and outside-directed carrier-mediated transport. *J. Pharm. Sci.* **89,** 63–75 (2000).

70. B??duneau, A. *et al.* A tunable Caco-2/HT29-MTX co-culture model mimicking variable permeabilities of the human intestine obtained by an original seeding procedure. *Eur. J. Pharm. Biopharm.* **87,** 290–298 (2014).

71. Castro, P., Madureira, R., Sarmento, B. & Pintado, M. *Concepts and Models for Drug Permeability Studies*. *Concepts and Models for Drug Permeability Studies* (2016). doi:http://dx.doi.org/10.1016/B978-0-08-100094-6.00012-2

72. Clark, M. A., Jepson, M. A. & Hirst, B. H. Exploiting M cells for drug and vaccine delivery. *Adv. Drug Deliv. Rev.* **50,** 81–106 (2001).

73. Kernéis, S. *et al.* Molecular studies of the intestinal mucosal barrier physiopathology using cocultures of epithelial and immune cells: A technical update. *Microbes Infect.* **2,** 1119–1124 (2000).

74. Kerneis, S., Bogdanova, A., Kraehenbuhl, J. & Pringault, E. Conversion by Peyer9s Patch Lymphocytes of Human Enterocytes into M Cells that ran sport Bacteria. **277,** 949–952 (1996).

75. Gullberg, E. *et al.* Expression of Specific Markers and Particle Transport in a New Human Intestinal M-Cell Model. *Biochem. Biophys. Res. Commun.* **279,** 808–813 (2000).

76. Debard, N., Sierro, F., Browning, J. & Kraehenbuhl, J. P. Effect of mature lymphocytes and lymphotoxin on the development of the follicle-associated epithelium and M cells in mouse peyer's patches. *Gastroenterology* **120,** 1173–1182 (2001).

77. Rieux, A. Des *et al.* Transport of nanoparticles across an in vitro model of the human intestinal follicle associated epithelium. *Eur. J. Pharm. Sci.* **25,** 455–465 (2005).

78. Ensign, L. M., Schneider, C., Suk, J. S., Cone, R. & Hanes, J. Mucus penetrating nanoparticles: Biophysical tool and method of drug and gene delivery. *Adv. Mater.* **24,** 3887–3894 (2012).

79. Ponchel, G. & Irache, J. M. Specific and non-specific bioadhesive particulate systems for oral delivery to the gastrointestinal tract. *Adv. Drug Deliv. Rev.* **34,** 191–219 (1998).

80. Woodley, J. New Possibilities for Drug Administration ? **40,** 77–84 (2001).

81. Fantini, J. *et al.* Spontaneous and induced dome formation by two clonal cell populations derived from a human adenocarcinoma cell line, HT29. *J. Cell Sci.* **83,** 235–49 (1986).

82. Lesuffleur, T., Barbat, A., Dussaulx, E. & Zweibaum, A. Growth Adaptation to Methotrexate of HT-29 Human Colon Carcinoma Cells Is Associated with Their Ability to Differentiate into Columnar Absorptive and Mucus-secreting Cells. *Cancer Res.* **50,** 6334–6343 (1990).

83. Walter, E., Janich, S., Roessler, B. J., Hilfinger, J. M. & Amidon, G. L. HT29-MTX/Caco-2 cocultures as an in vitro model for the intestinal epithelium: In vitro-in vivo correlation with permeability data from rats and humans. *J. Pharm. Sci.* **85,** 1070–1076 (1996).

84. Behrens, I., Stenberg, P., Artursson, P. & Kissel, T. Transport of lipophilic drug molecules in a new mucus-secreting cell culture model based on HT29-MTX cells. *Pharm. Res.* **18,** 1138–1145 (2001).

85. Kheradmandnia, S., Vasheghani-Farahani, E., Nosrati, M. & Atyabi, F. Preparation and characterization of ketoprofen-loaded solid lipid nanoparticles made from beeswax and carnauba wax. *Nanomedicine Nanotechnology, Biol. Med.* **6,** 753–759 (2010).

86. Dohrn, R., Bertakis, E., Behrend, O., Voutsas, E. & Tassios, D. Melting point depression by using supercritical CO2for a novel melt dispersion micronization process. *J. Mol. Liq.* **131–132,** 53–59 (2007).

87. Buchwald, R., Breed, M. D. & Greenberg, A. R. The thermal properties of beeswaxes: unexpected findings. *J. Exp. Biol.* **211,** 121–127 (2008).

88. Rodríguez-Rojo, S. *et al.* Encapsulation of perfluorocarbon gases into lipid-based carrier by PGSS. *J. Supercrit. Fluids* **82,** 206–212 (2013).

89. Gonçalves, V. S. S., Matias, A. A., Rodríguez-Rojo, S., Nogueira, I. D. & Duarte, C. M. M. Supercritical fluid precipitation of ketoprofen in novel structured lipid carriers for enhanced mucosal delivery - A comparison with solid lipid particles. *Int. J. Pharm.* **495,** 302–311 (2015).

90. Minekus, M. *et al.* A standardised static *in vitro* digestion method suitable for food – an international consensus. *Food Funct.* **5,** 1113–1124 (2014).

91. Schimpel, C. *et al.* Development of an advanced intestinal in vitro triple culture permeability model to study transport of nanoparticles. *Mol. Pharm.* **11,** 808–818 (2014).

92. Serra, A. T. *et al.* Processing cherries (Prunus avium) using supercritical fluid technology. Part 2. Evaluation of SCF extracts as promising natural chemotherapeutical agents. *J. Supercrit. Fluids* **55,** 1007–1013 (2011).

93. Membrane, R. T. *et al.* Transwell ® Permeable Supports Selection and Use Guide. (2007).

94. Hidalgo, I. J., Raub, T. J. & Borchardt, R. T. Characterization of the Human Colon Carcinoma Cell Line (Caco-2) as a Model System for Intestinal Epithelial Permeability. *Gastroenterology* **96,** 736–749 (1989).

95. Bernal, J. L., Jiménez, J. J., Del Nozal, M. J., Toribio, L. & Martín, M. T. Physico-chemical parameters for the characterization of pure beeswax and detection of adulterations. *Eur. J. Lipid Sci. Technol.* **107,** 158–166 (2005).

96. Lian, Z., Epstein, S. A., Blenk, C. W. & Shine, A. D. Carbon dioxide-induced melting point depression of biodegradable semicrystalline polymers. *J. Supercrit. Fluids* **39,** 107–117 (2006).

97. Lundstedt, T. *et al.* Experimental design and optimization. *Chemom. Intell. Lab. Syst.* **42,** 3–40 (1998).

98. Vezzú, K. *et al.* Production of lipid microparticles containing bioactive molecules functionalized with PEG. *J. Supercrit. Fluids* **54,** 328–334 (2010).

99. Mandžuka, Z. & Knez, Ž. Influence of temperature and pressure during PGSS™ micronization and storage time on degree of crystallinity and crystal forms of monostearate and tristearate. *J. Supercrit. Fluids* **45,** 102–111 (2008).

100. Alessi, P. *et al.* Particle Production of Steroid Drugs Using Supercritical Fluid Processing. *Ind. Eng. Chem. Res.* **35,** 4718–4726 (1996).

101. K. Vezzù, A. B. Solid–Liquid Equilibria of Multicomponent Lipid Mixtures Under CO2 Pressure: Measurement and Thermodynamic Modeling. *VTT Publ.* (2008). doi:10.1002/aic.11543

102. Rabinow, B. E. Nanosuspensions in drug delivery. *Nat. Rev. Drug Discov.* **3,** 785–796 (2004).

103. Ranjan, A. P., Mukerjee, A., Helson, L. & Vishwanatha, J. K. Scale up, optimization and stability analysis of Curcumin C3 complex-loaded nanoparticles for cancer therapy. *J. Nanobiotechnology* **10,** 1–18 (2012).

104. Saldanha Do Carmo, C. *et al.* Formulation of pea protein for increased satiety and improved foaming properties. *RSC Adv.* **6,** 6048–6057 (2016).

105. Pedro, A. S. *et al.* Curcumin-loaded solid lipid particles by PGSS technology. *J. Supercrit. Fluids* **107,** 534–541 (2016).

106. Yuan, Y., Gao, Y., Zhao, J. & Mao, L. Characterization and stability evaluation of β-carotene nanoemulsions prepared by high pressure homogenization under various emulsifying conditions. *Food Res. Int.* **41,** 61–68 (2008).

107. Freitas, C. & Müller, R. H. Effect of light and temperature on zeta potential and physical stability in solid lipid nanoparticle (SLN®) dispersions. *Int. J. Pharm.* **168,** 221–229 (1998).

108. Wiacek, A. & Chibowski, E. Zeta potential, effective diameter and multimodal size distribution in oil/water emulsion. *Colloids Surfaces A Physicochem. Eng. Asp.* **159,** 253–261 (1999).

109. Paradkar, A., Ambike, A. A., Jadhav, B. K. & Mahadik, K. R. Characterization of curcumin-PVP solid dispersion obtained by spray drying. *Int. J. Pharm.* **271,** 281–286 (2004).

110. Zabihi, F., Xin, N., Jia, J., Chen, T. & Zhao, Y. High yield and high loading preparation of curcumin-PLGA nanoparticles using a modified supercritical antisolvent technique. *Ind. Eng. Chem. Res.* **53,** 6569–6574 (2014).

111. Jantarat, C. *et al.* Curcumin-Hydroxypropyl-β-Cyclodextrin Inclusion Preparation Methods Effect of Common Solvent Evaporation, Freeze Drying, dan pH Shift on Solubility and Stability of Curcumin.pdf. *Trop. J. Pharm. Res.* **13,** 1215–1223 (2004).

112. Sari, T. P. *et al.* Preparation and characterization of nanoemulsion encapsulating curcumin. *Food Hydrocoll.* **43,** 540–546 (2015).

113. des Rieux, A. *et al.* Helodermin-loaded nanoparticles: Characterization and transport across an in vitro model of the follicle-associated epithelium. *J. Control. Release* **118,** 294–302 (2007).

114. Malich, G., Markovic, B. & Winder, C. The sensitivity and specificity of the MTS tetrazolium assay for detecting the in vitro cytotoxicity of 20 chemicals using human cell lines. *Toxicology* **124,** 179–192 (1997).

115. Mohanty, C. & Sahoo, S. K. The in vitro stability and in vivo pharmacokinetics of curcumin prepared as an aqueous nanoparticulate formulation. *Biomaterials* **31,** 6597–6611 (2010).

116. Guri, A., Gülseren, I. & Corredig, M. Utilization of solid lipid nanoparticles for enhanced delivery of curcumin in cocultures of HT29-MTX and Caco-2 cells. *Food Funct.* **4,** 1410 (2013).

117. Yang, Y., Xiao, H. & McClements, D. J. Impact of Lipid Phase on the Bioavailability of Vitamin E in Emulsion-Based Delivery Systems: Relative Importance of Bioaccessibility, Absorption, and Transformation. *J. Agric. Food Chem.* **65,** 3946–3955 (2017).

118. Jun, H. S., Bae, G., Ko, Y. T. & Oh, Y. S. Cytotoxicity and biological efficacy of exendin-4-encapsulated solid lipid nanoparticles in INS-1 cells. *J. Nanomater.* **2015,** 1–7 (2015).

119. Scientific, E. *et al.* Technical Section. **33,** 484–489 (1984).

120. Owen, R. L. & Jones, A. L. Epithelial Cell Specialization within Human Peyer's Patches: An Ultrastructural Study of Intestinal Lymphoid Follicles. *Gastroenterology* **66,** 189–203 (1974).

121. Foss, A. C. & Peppas, N. A. Investigation of the cytotoxicity and insulin transport of acrylic-based copolymer protein delivery systems in contact with caco-2 cultures. *Eur. J. Pharm. Biopharm.* **57,** 447–455 (2004).

122. Lubben, I. M. V. A. N. D. E. R. *et al.* Transport of Chitosan Microparticles for Mucosal Vaccine Delivery in a Human Intestinal M-cell Model. **10,** 449–456 (2002).

123. Wahlang, B., Pawar, Y. B. & Bansal, A. K. Identification of permeability-related hurdles in oral delivery of curcumin using the Caco-2 cell model. *Eur. J. Pharm. Biopharm.* **77,** 275–282 (2011).

124. Dempe, J. S., Scheerle, R. K., Pfeiffer, E. & Metzler, M. Metabolism and permeability of curcumin in cultured Caco-2 cells. *Mol. Nutr. Food Res.* **57,** 1543–1549 (2013).

125. Carr, D. A. & Peppas, N. A. Assessment of poly(methacrylic acid-co-N-vinyl pyrrolidone) as a carrier for the oral delivery of therapeutic proteins using Caco-2 and HT29-MTX cell lines. *J. Biomed. Mater. Res. - Part A* **92,** 504–512 (2010).

126. Sao Pedro, A. Supercritical fluid technology for development of solid lipid particles entrapping curcumin. 102 (2016).

127. Abreu, M. T. Toll-like receptor signalling in the intestinal epithelium: How bacterial recognition shapes intestinal function. *Nat. Rev. Immunol.* **10,** 131–143 (2010).

128. Hubatsch, I., Ragnarsson, E. G. E. & Artursson, P. Determination of drug permeability and prediction of drug absorption in Caco-2 monolayers. *Nat. Protoc.* **2,** 2111–2119 (2007).

7. Appendix

Appendix A – Supercritical fluids properties.

Table 7.1| Critical Properties of Fluids of Interest in Supercritical Processes. [35]

Fluid	Critical Temperature (°C)	Critical Pressure (bar)	Critical Volume ($cm^3 \cdot mol^{-1}$)
CO2	30.97	73.7	94.07
Ethane	32.15	48.7	145.5
Propane	96.65	42.5	200.0
Water	373.95	220.6	55.95
Ammonia	132.25	113.5	72.47
n-Hex			0
Metha			0

Table 7.2| physicochemical properties of fluids and supercritical fluids. [37]

	Density ($Kg.m^{-3}$)	Viscosity (mPa.s)	Diffusivity ($cm^2.s^{-1}$)
Gas	0.8-1.3	0.01-0.03	0.1-0.2
Liquid	800-1200	0.4-1.1	0.00001-0.0001
SCF	300-1000	0.05-0.01	0.0001-0.001

Appendix B – High-performance liquid chromatography

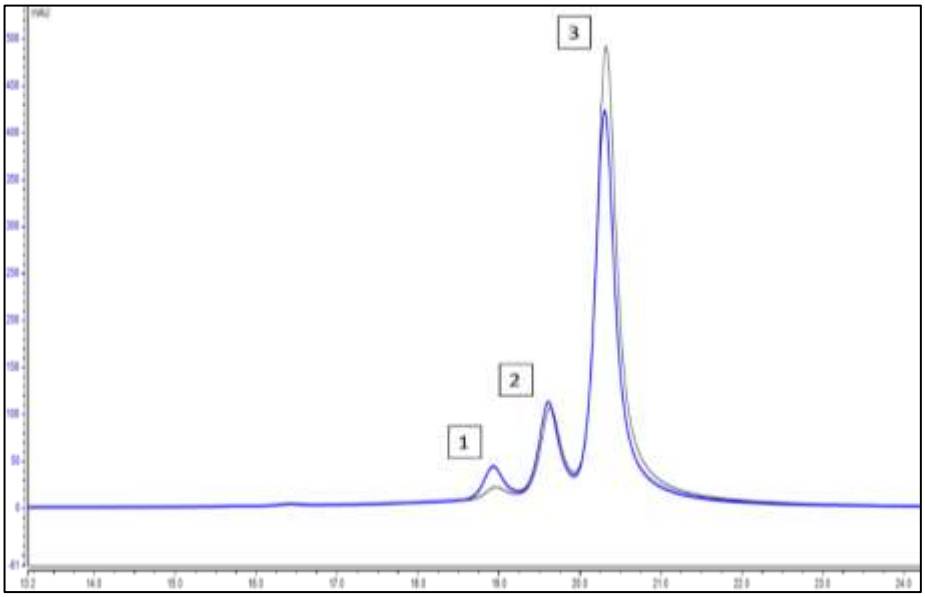

Figu **gma**
(blue s: 1)
bisd

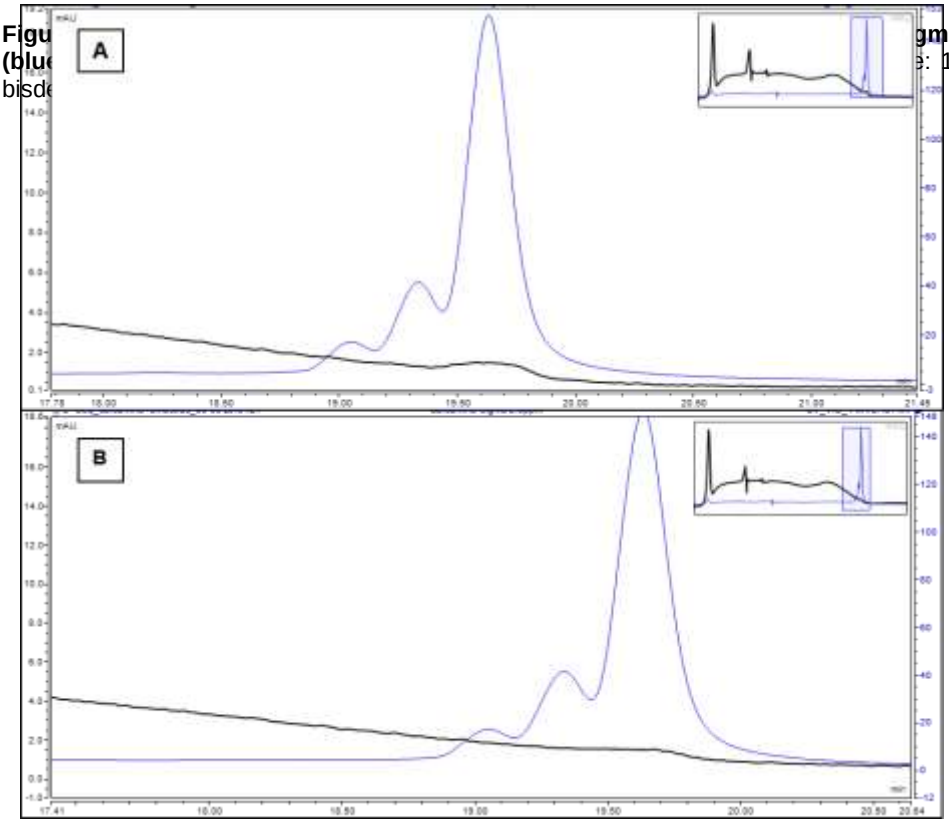

Figure 7.2| Curcumin permeation studies at 420 nm. A) Permeated curcumin in a Co-culture model and B) in a Caco-2 model, after 4 h incubation at 37 °C in a humidified atmosphere of 5 % CO2.

Appendix C – Curcumin permeability studies – TEER values

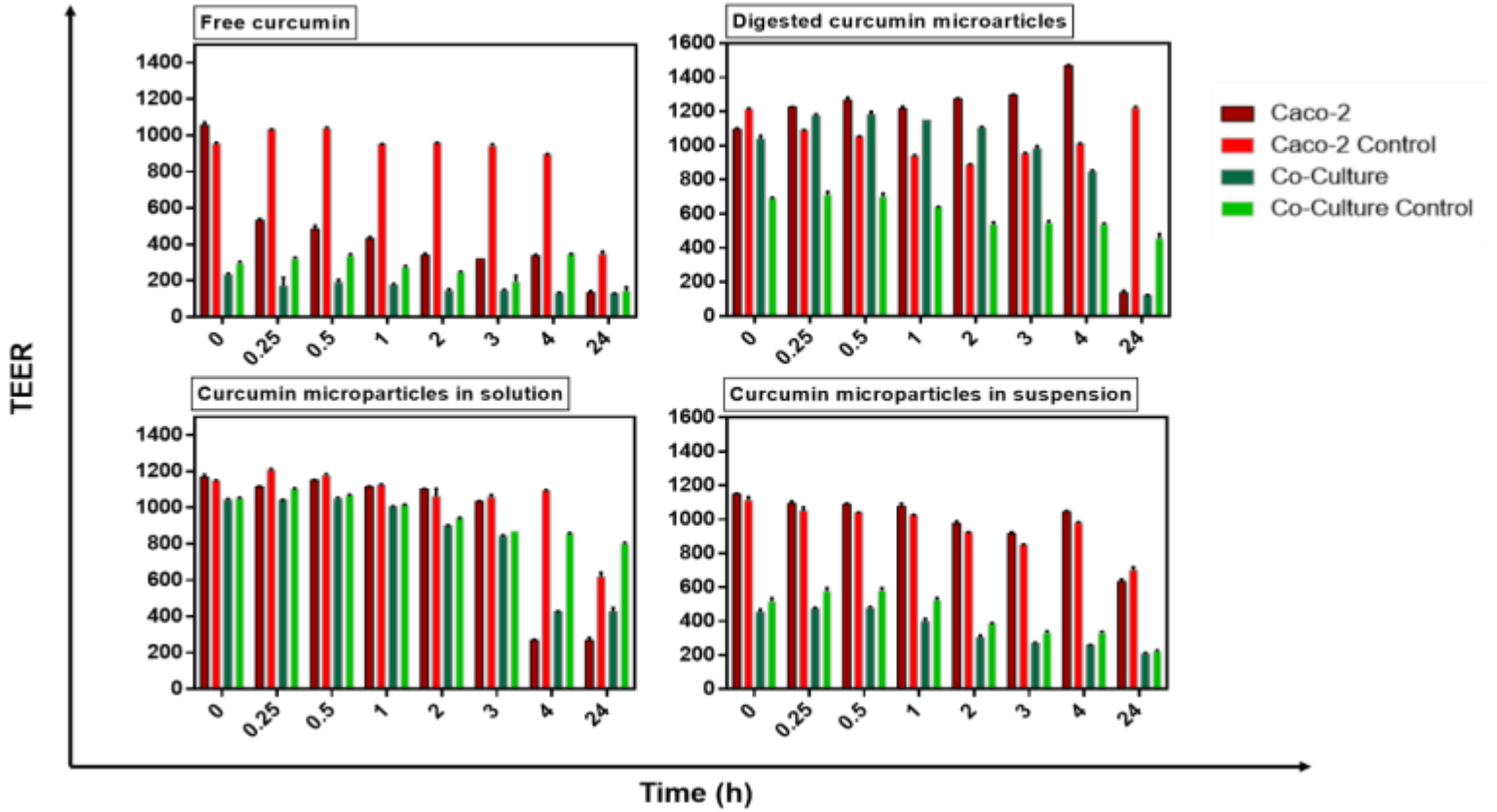

Figure 7.3| TEER values from curcumin permeation assay. The tests occurred for 24 hours and the values presented were a mean of 3 measurements per well. The permeability was tested on inserts with differentiated Caco-2 cells, as well as on the triple co-culture implemented.